The High Energy Solar Spectroscopic Imager

Step Two MIDEX Proposal

Volume I

Investigation and Technical Plan

HESSI

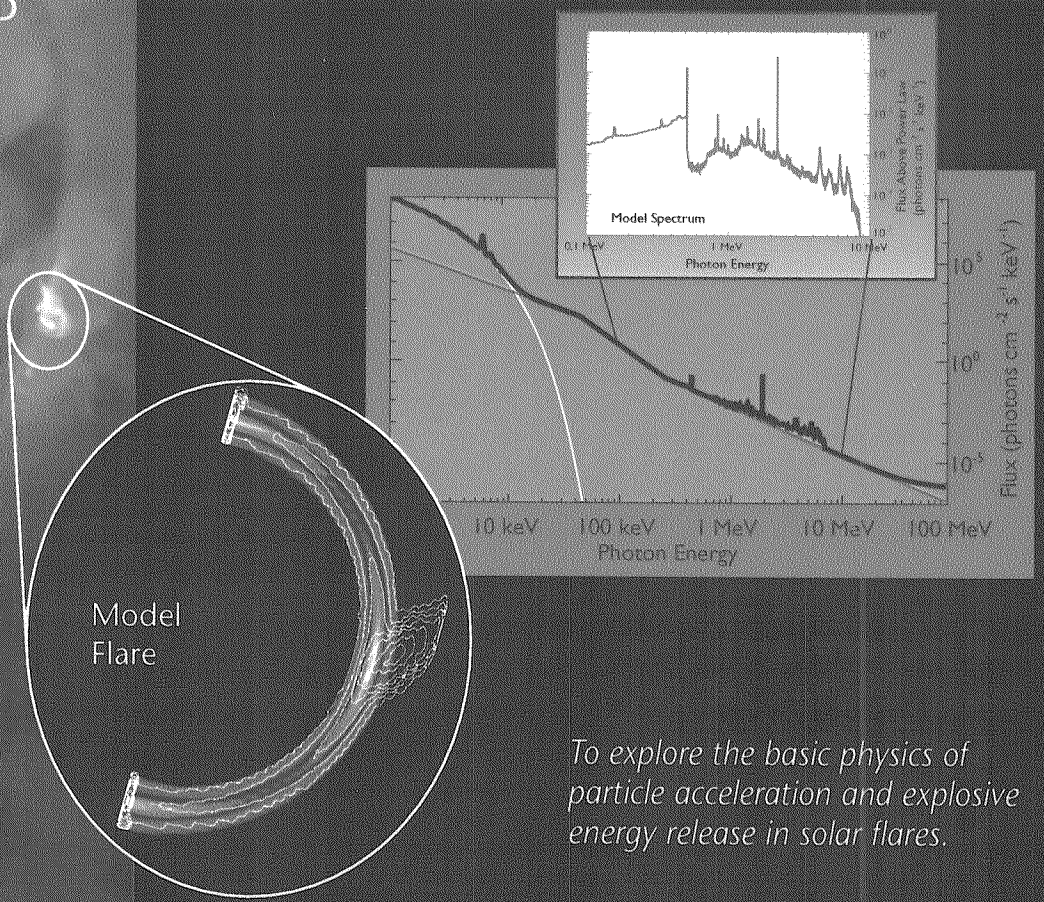

To explore the basic physics of particle acceleration and explosive energy release in solar flares.

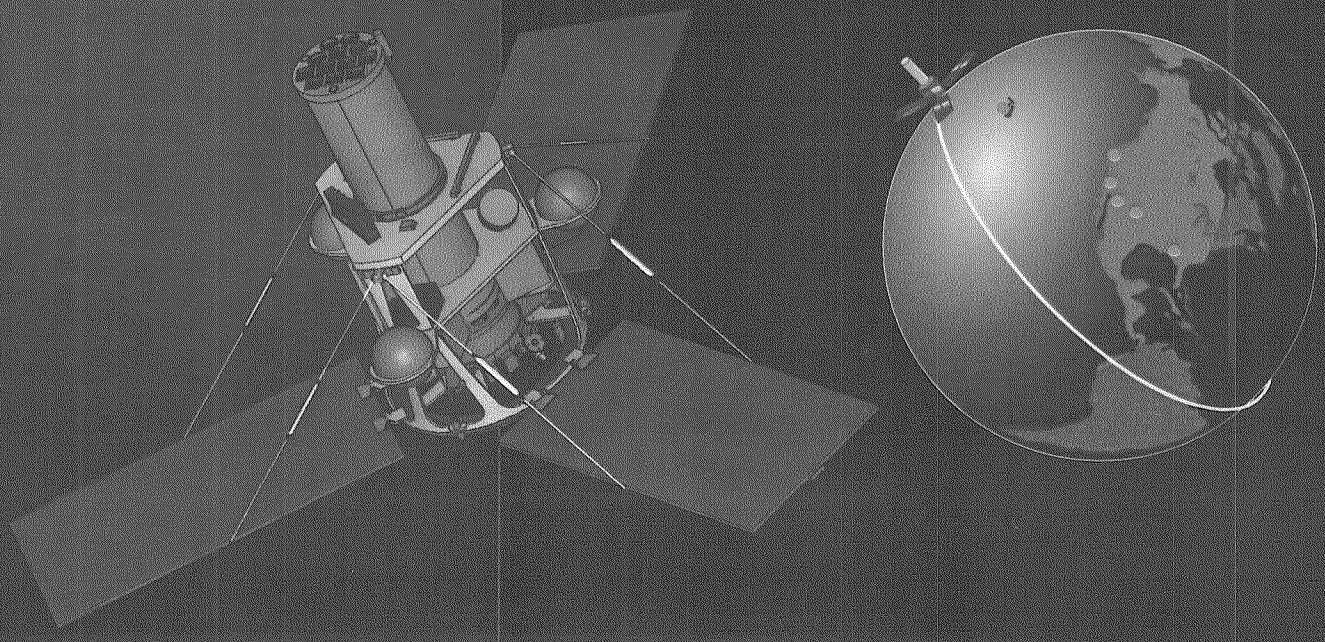

UNIVERSITY OF CALIFORNIA, BERKELEY

BERKELEY • DAVIS • IRVINE • LOS ANGELES • RIVERSIDE • SAN DIEGO • SAN FRANCISCO

SANTA BARBARA • SANTA CRUZ

OFFICE OF THE VICE CHANCELLOR FOR RESEARCH
TELEPHONE: (510) 642-7540
FACSIMILE: (510) 643-5620

BERKELEY, CALIFORNIA 94720

June 21, 1995

Dr. Wesley T. Huntress, Jr.
Associate Administrator
for Space Science
NASA Headquarters
Washington, D.C. 20546

Dear Dr. Huntress,

On behalf of the University of California at Berkeley, I am pleased to support the "High Energy Solar Spectroscopic Imager (HESSI)" investigation proposed by Professor Robert P. Lin in response to Announcement of Opportunity no. 95-OSS-02.

We look forward to working with NASA on this exciting scientific project.

Sincerely,

Joseph Cerny
Vice Chancellor for Research

National Aeronautics and
Space Administration

Goddard Space Flight Center
Greenbelt, MD 20771

Reply to Attn of: 600

DEC 15 1995

Professor Robert P. Lin
Space Sciences Laboratory
University of California
Berkeley, CA 94720-7450

Dear Professor Lin:

The Space Sciences and Engineering Directorates of the Goddard Space Flight Center are committed to participating with you at the Space Sciences Laboratory of the University of California, Berkeley, in building the High Energy Solar Spectroscopic Imager (HESSI) within the cost and programmatic constraints of the Medium-class Explorer (MIDEX) program as specified in the Announcement of Opportunity (AO-95-OSS-02).

Our scientific and technical staff has worked closely with scientists and engineers at Berkeley over the last five years to conceive and develop an exceptional high-energy instrument that incorporates the best of the Goddard and Berkeley programs. Our scientific and engineering expertise in solar hard X-ray observations extends from the early Orbiting Solar Observatories in the 1960's and 1970's, through the Solar Maximum Mission (SMM) in the 1980's, and includes, most recently, the balloon flight of the High Energy Imaging Device (HEIDI) in 1993, and the fabrication of a Telescope Demonstration Unit that is now undergoing extensive tests. Our theory program led by Drs. Holman and Ramaty is internationally renowned as the finest in the field. In addition, we can offer our unique engineering expertise in cryogenics and thermal design that is crucial for the instrumentation being proposed.

The combination of scientific and technical abilities at Goddard nicely complements the capabilities of your team at Berkeley. There, you have developed expertise in high resolution solar X-ray and gamma-ray spectroscopy based on your germanium detector technology. You have had many balloon flights of such detectors over the last two decades, culminating in three long-duration flights in the Antarctic of your High Resolution Gamma-ray and Hard X-ray Spectrometer, the most recent in January, 1995. Thus, by combining Goddard's X-ray imaging and cryogenics talents with your high resolution spectroscopy capabilities, we will produce the best High Energy Solar Spectroscopic Imager at the lowest possible cost.

Our ability to work successfully with the scientists and engineers at Berkeley has been amply demonstrated with many missions, including, most recently, the Fast Auroral Snapshot Explorer (FAST) Small Explorer (SMEX) program, all of which have been done within cost and schedule. One difference in our proposed involvement with HESSI, compared to previous joint ventures, is that, in this case, we have agreed to contribute roughly half of the instrument development

effort with the overall HESSI management residing at Berkeley. We believe that this is the most efficient mode of operation, given that the PI is also located at Berkeley. We look forward to participating in this mode and will provide you with the necessary support to ensure the success of the endeavor at the lowest possible cost.

We strongly endorse the participation of our leading astrophysicists, Drs. Crannell, Davila, Dennis, Desai, Holman, Orwig, Ramaty, Tueller, and von Rosenvinge, as Co-Investigators and Associated Scientists on this proposal. In addition, we will fully support Associated Scientists employed by other organizations while they are working on-site at Goddard. Currently, these scientists are Drs. Aschwanden, Schmahl, Schwartz, and Zarro. We recognize the crucial role of Co-investigator, Dr. Gordon Hurford from the California Institute of Technology, in the design and development of the imaging part of HESSI, and we will welcome his full-time participation at Goddard for the duration of the HESSI program.

In addition to the scientific personnel listed above, we will fully support the Goddard management and engineering team necessary to meet our obligations, as outlined in the proposal. The required personnel and facilities are available and will be committed to HESSI if and when this proposal is accepted. As you are aware, Goddard has an excellent record of providing the civil servant manpower planned for projects and we will commit to do so for HESSI.

With the combined expertise of the Goddard Space Flight Center and the University of California, Berkeley, we are very excited about the prospect of building a superb X-ray and gamma-ray imaging spectrometer. We look forward with keen anticipation to the time when that instrument will make high fidelity X-ray and gamma-ray movies of solar flares that will both excite the general public and provide a deeper scientific understanding of the largest explosions in our solar system.

Sincerely,

Stephen S. Holt
Director of Space Sciences

Allan Sherman
Director of Engineering

Approval:

Joseph H. Rothenberg
Director

Date

Proposal #
NASA Use Only

Medium - Class Explorer (MIDEX)
Investigation Summary Form

PRINCIPAL INVESTIGATOR			
Prof. Robert P. Lin			
INSTITUTION			
University of California, Berkeley			
DEPARTMENT			
Space Sciences Laboratory			
ADDRESS / STREET			
Centennial Drive at Grizzly Peak Boulevard			
CITY / TOWN	STATE	ZIP / POSTAL CODE	COUNTRY
Berkeley	CA	94720-7450	U.S.A.
TELEPHONE	FAX	E-MAIL ADDRESS	
(510) 642-1149	(510) 643-8302	boblin@sunspot.ssl.berkeley.edu	

INVESTIGATION TITLE

HIGH ENERGY SOLAR SPECTROSCOPIC IMAGER (HESSI)

INVESTIGATION ABSTRACT HESSI will investigate the physics of particle acceleration and energy release in solar flares. Observations will be made of X-rays and gamma rays from 2 keV to 20 MeV with an unprecedented combination of high resolution imaging and spectroscopy. It uses Fourier-transform imaging with 12 bi-grid modulation collimators and cooled germanium and silicon detectors mounted on a Sun-pointed spin-stabilized spacecraft in a low-altitude equatorial orbit. HESSI will provide the first imaging spectroscopy in hard X-rays with 2 arcsec angular resolution, time resolution to tens of ms, and <1 keV energy resolution; the first gamma-ray line spectroscopy with ~1 keV energy resolution; and the first gamma-ray line and continuum imaging with 20 arcsec angular resolution. HESSI is ideally launched by the year 2000, in time to detect the thousands of flares expected during the next solar maximum.

DISCIPLINE AREA (CHECK AS APPLY)

[ ] SPACE PHYSICS
- [ ] IONOSPHERIC
- [ ] MESOSPHERIC
- [ ] THERMOSPHERIC
- [ ] COSMIC
- [ ] MAGNETOSPHERIC
- [ ] HELIOSPHERIC
- [X] SOLAR

[ ] ASTROPHYSICS
- [ ] RADIO
- [ ] INFRARED
- [ ] SUBMILLIMETER
- [ ] OPTICAL
- [ ] ULTRAVIOLET
- [ ] X-RAY
- [ ] GAMMA-RAY
- [ ] GRAVITY

SPACECRAFT MODE (CHECK ONE)

[X] NASA-PROVIDED [ ] PI-MODE

TOTAL BUDGET AMOUNT (EXCLUDING MO&DA)

$ 39,400,000*

TOTAL MO & DA BUDGET

$ 15,000,000

*$39,800,000 for 22-month definition phase program.

Proposal #
NASA Use Only

PRINCIPAL INVESTIGATOR

Prof. Robert P. Lin

INVESTIGATION TITLE

HIGH ENERGY SOLAR SPECTROSCOPIC IMAGER (HESSI)

LIST OF CO-INVESTIGATORS at Other Institutions

NAME	INSTITUTION
Dr. Brian R. Dennis	NASA Goddard Space Flight Center
Dr. Carol Jo Crannell	NASA Goddard Space Flight Center
Dr. Gordon D. Holman	NASA Goddard Space Flight Center
Dr. Reuven Ramaty	NASA Goddard Space Flight Center
Dr. Tycho T. von Rosenvinge	NASA Goddard Space Flight Center
Prof. Richard C. Canfield	Montana State University
Dr. Hugh S. Hudson	Solar Physics Research Corporation
Dr. James C. Ling	Jet Propulsion Laboratory
Prof. A. Gordon Emslie	University of Alabama in Huntsville
Dr. Patricia L. Bornmann	National Oceanic and Atmospheric Administration
Mr. Norman W. Madden	Lawrence Berkeley National Laboratory
Dr. Gordon J. Hurford	California Institute of Technology*
Prof. Arnold Benz	Institute of Astronomy ETHZ, Switzerland
Prof. John C. Brown	University of Glasgow, Scotland, U.K.
Dr. Shinzo Enome	National Astronomical Observatory, Japan
Dr. Takeo Kosugi	National Astronomical Observatory, Japan
Prof. H. Frank van Beek	Delft University of Technology, Netherlands
Dr. Nicole Vilmer	Observatoire de Paris-Meudon, France

*currently at Caltech; institutional affiliation for project participation to be determined.

INSTITUTIONAL ENDORSEMENT

INSTITUTION NAME

The Regents of the University of California, Berkeley

NAME AND TITLE OF AUTHORIZING OFFICIAL

Joyce B. Freedman
Director, Sponsored Projects Office†

SIGNATURE Joyce Freedman DATE 12/14/95

†Sponsored Projects Office, 336 Sproul Hall, University of California, Berkeley, CA 94720-5940.
For NASA matters: tel. (510) 642-8109; fax (510) 642-8236; e-mail pgates@uclink3.berkeley.edu.

HESSI Step-Two Proposal

Volume I: Investigation and Technical Plan

Volume II: Management Plan

Volume III: Cost Plan

(see Volume III for detailed Table of Contents)

1. SCIENCE INVESTIGATION & INVESTIGATION PLAN

The primary scientific objective of the High Energy Solar Spectroscopic Imager (HESSI) is to understand particle acceleration and explosive energy release in the magnetized plasmas at the Sun, processes which also occur at many other sites in the universe. The Sun is the most powerful particle accelerator in the solar system, accelerating ions up to tens of GeV and electrons to hundreds of MeV. Solar flares are the most powerful explosions, releasing up to 10^{32}-10^{33} ergs in 100-1000 s. The accelerated 10-100 keV electrons (and perhaps $\gtrsim 1$ MeV ions) appear to contain the bulk of this energy, indicating that the particle acceleration and energy release processes are intimately linked. How the Sun releases this energy, and how it rapidly accelerates electrons and ions with such high efficiency and to such high energies, is presently unknown.

Hard X-ray/γ-ray continuum and γ-ray lines are the most direct signatures of the energetic electrons and ions, respectively. **HESSI will provide the first hard X-ray imaging spectroscopy, the first high-resolution spectroscopy of solar γ-ray lines, the first imaging above 100 keV, and the first imaging of solar γ-ray lines.** HESSI combines a Fourier-transform imaging system with a high-resolution spectrometer spanning energies from soft X-rays (2 keV) to high-energy γ-rays (20 MeV) with a common set of optics (see foldout at back of volume). HESSI's hard X-ray imaging spectroscopy provides spectral resolution of ~1 keV, spatial resolution down to 2 arcsec, and temporal resolution as short as tens of milliseconds. **These parameters are, for the first time, commensurate with physically relevant scales for energy loss and transport of the tens-of-keV electrons that are believed to contain much of the energy released in the flare.**

HESSI's γ-ray imaging spectroscopy will provide **the first imaging of energetic protons, heavy ions and relativistic electrons; the first information on the angular distribution of accelerated ions; and detailed information on elemental abundances for both the ambient plasma and the accelerated ions.**

HESSI will also provide **hard X-ray imaging of the Crab Nebula with a spatial resolution down to 2 arcsec,** and will continuously monitor a large fraction of the sky to provide **high spectral resolution observations of transient hard X-ray and γ-ray sources, including accreting black holes and cosmic γ-ray bursts.** For these, the confirmation and detailed study of possible line and continuum features may provide the crucial information for determining their origin.

HESSI has a full-Sun field of view and a solid-state memory big enough to hold all the data from the largest flare, so that pointing and mission operations can be automated. It will utilize spacecraft subsystems from the FAST Small Explorer with only minor modifications, for a simple, reliable, and inexpensive NASA-provided, Sun-pointed spinning spacecraft. A 600-km equatorial orbit minimizes background and radiation damage to the germanium detectors.

The solar activity cycle is predicted to peak in the year 2000. Thus, a HESSI launch at the end of 1999 would be ideal, but a launch as late as the end of 2001 would be acceptable. A two-year nominal mission (a third year highly desirable) will provide observations of tens of thousands of microflares, thousands of hard X-ray flares, and hundreds of γ-ray line flares.

The HESSI team includes leading experts in solar high-energy spectroscopy and imaging, with decades of hardware and data analysis experience. The extensive heritage from the UCB HIREGS and the GSFC HEIDI balloon programs, and the UCB/GSFC FAST SMEX program, plus recent technology development efforts, make HESSI ready to be built within MIDEX cost and schedule constraints.

The HESSI mission includes **a combination of space- and ground-based observations to provide the critical context information** required for theoretical interpretation and detailed modeling. Rapid and direct access by the solar scientific community to the HESSI data and analysis software, together with a **Guest Investigator program funded from HESSI MO&DA funds,** will ensure the maximum scientific return from this comprehensive data set.

1.a. UPDATE TO SCIENTIFIC OBJECTIVES

There are no changes to the HESSI objectives given in Step-One. Since then, however, new results have appeared which make HESSI even more compelling. Share and Mur-

phy (1995) showed that the 1.634 MeV ^{20}Ne line is unexpectedly enhanced in SMM γ-ray line flares. This effect appears to be due to large fluxes of low-energy ions with a total energy content perhaps comparable to that in accelerated electrons, rather than to an overabundance of neon (Ramaty *et al.* 1995). HESSI will provide the first high-resolution spectroscopy and imaging of the ^{20}Ne line, together with simultaneous ground-based imaging measurements of linear polarization in the Hα line produced by beams of ≳0.1 MeV protons (Metcalf *et al.*,1994). Thus, **for the first time, the partition of energy between accelerated electrons (derived from hard X-ray measurements) and ions can be measured.**

2. TECHNICAL APPROACH

2.a. MISSION DESIGN

The HESSI **Baseline Mission** (see foldout tables and schematic) involves a single instrument consisting of an Imaging System, a Spectrometer, and an Instrument Data Processing Unit (IDPU) containing all the instrument electronics. The Imaging System consists of 12 Rotating Modulation Collimators (RMCs), each consisting of a pair of widely separated grids mounted on a rotating spacecraft (see Figure 2.b.1 and foldout drawing) The grids are planar arrays of equally spaced X-ray-opaque slats separated by transparent slits. The Spectrometer consists of 12 germanium detectors (GeDs) and 12 silicon detectors (SiDs), one of each behind each RMC, to provide high spectral resolution measurements from ~10 keV to 20 MeV and ~2-20 keV, respectively (see table in foldout). As the spacecraft rotates, the RMCs convert the spatial information into temporal modulation of the photon counting rates of the GeDs and SiDs. The GeDs are cooled to <85K, and the SiDs to ~140K, by a space-qualified long-life mechanical cooler.

The energy and arrival time of every photon, together with pointing information from the Solar Aspect System (SAS) and Roll Angle System (RAS), are recorded in the IDPU's solid-state memory (large enough to hold all the data from the largest flare) and automatically telemetered once per orbit down to the ground station. With these data the X-ray/γ-ray images can be reconstructed on the ground (see example in foldout). The instrument's ~1° field of view is much wider than the ~0.5° solar diameter, so pointing can be automated.

We propose that a Sun-pointed, spin-stabilized spacecraft, consisting mostly of subsystems already developed for the FAST and SWAS SMEX missions, be provided by NASA.

The Baseline Mission's 600-km altitude, equatorial orbit skirts the South Atlantic Anomaly (SAA) to minimize both background and radiation damage to the GeDs while providing a three-year minimum orbit lifetime. A single near-equatorial ground station will provide full command and telemetry coverage every orbit.

For the Step-One proposal, the information provided to us by the MIDEX office indicated that the Med-Lite launch vehicle could achieve this orbit with ±10 km altitude dispersion. Subsequently, however, we have learned that the 3σ dispersion in altitude for an equatorial orbit is actually ±350 km. Thus, for the Baseline Mission, a spacecraft propulsion system has been added to correct for this dispersion.

Minimum Science Mission (MSM). A 600±20-km altitude, ~7.5°-inclination orbit, which is achievable with the standard Med-Lite launch vehicle without a spacecraft propulsion system, is adequate for the MSM. The fluence of >30 MeV SAA protons in the two-year MSM duration is still a factor of two below that for the GeDs to exhibit noticeable radiation damage. However, ~5% of the observing time is lost due to SAA passages.

The number of RMCs, GeDs and SiDs, would be reduced for the MSM from twelve to seven, and some grids would be thinner (see Table 2.b.3). The finest grid pair would be eliminated, thus relaxing the tolerances on grid twist maintenance and aspect determination by a significant factor, ~1.5. The weight, power, and cooling are significantly reduced (foldout). The telemetry requirements are reduced by a factor of 7/12 so a single near-equatorial ground station can still provide full coverage for the 7.5°-inclination orbit.

The Minimum Science Mission preserves the critical defining elements of HESSI: (1) hard and soft X-ray imaging spectroscopy with a few arcsec angular resolution and ~1 keV energy resolution, (2) high-resolution (~1 keV) γ-ray line spectroscopy, and (3) γ-ray line and continuum imaging. The primary science impacts are a significant, but acceptable, reduction in overall imaging capabilities, with a small loss of sensitivity for γ-ray line spectroscopy. The finest spatial reso-

lution for imaging spectroscopy would be 3 instead of 2 arcsec at energies $\lesssim$ 40 keV, 5 arcsec up to $\lesssim$ 200 keV, and 40 arcsec above 200 keV (Table 2.b.3). The image quality (dynamic range) is reduced by 20% since the number of Fourier components goes down by ~40%. The effective area and number of RMCs for imaging at γ-ray energies drops by a factor of 2. The total effective area is reduced by 40% at $\lesssim$ 35 keV, by 30% between 35 and 200 keV, but only 20% for γ-ray line spectroscopy.

Both the Baseline and Minimum Science Missions can achieve the HESSI scientific requirements with no new technology development. The required technology development has already been completed for grids, metering structure to hold the grids, aspect systems, detectors, coolers, electronics, etc. Furthermore, HESSI makes extensive use of subsystems already developed, fabricated, tested, and delivered for FAST, HEIDI, HIREGS, and other projects. Some ongoing technology developments which can provide enhanced performance (e.g., LIGA grids), or which can significantly simplify the instrument (e.g., Si drift detectors) appear very likely to be ready by the definition phase, but **these are not required for either the Baseline or Minimum Science Mission.** We plan to make final selection of all grids, detectors, coolers, etc., and have detailed designs for the entire mission ready at the end of the definition phase. The Minimum Science Mission will be studied during the definition phase to determine the potential cost, schedule, and spacecraft implications, and to define the decision points and criteria for descoping.

The **Mission Elements** are summarized in Table 2.a.1 and discussed below.

Mission Timeline. Launch will be from the Kennedy Space Center on a Med-Lite launch vehicle, with the detectors warm (cryocooler off) and the spacecraft power system, propulsion and heater control systems, and the C&DH internally powered on (40 watts max. total). Following the Delta 2nd-stage burn, the spacecraft is oriented and spun up to 55 rpm. The Star 37 kick motor is then fired at equator crossing to reduce the orbit inclination to <2.5°. Since the Star 37 is unguided, final orbit dispersions can be as much as ±350 km altitude (3σ) and ±0.2° inclination. The Star 37 is then jettisoned and the spacecraft despun to 2 rpm by a yo-yo deployment. The solar arrays are deployed. The Attitude Control System (ACS) torquer rods then turn the spacecraft to the Sun, guided by the fan Sun sensor, and spin it up to 15 rpm. The spacecraft hydrazine thrusters are commanded at appropriate times to eliminate the altitude dispersion by either raising the perigee or lowering the apogee.

Once the operational altitude, orientation and spin rates have been achieved, all other spacecraft systems will be turned on and checked out, followed by the instrument's IDPU, mechanical cooler, SAS, and RAS. An Intermediate Sun Sensor (ISS) provides inputs for the ACS transition from full sky coverage to the SAS. Once the Sun comes within 0.7° of the spin axis, the ACS uses direct error signals from the SAS, thus, making for fully-automated closed-loop pointing during orbit day.

Table 2.a.1. Mission Elements

1. Mission operations scenarios:	See Section 2.a.1.
2. Spacecraft pointing requirements:	Spinning spacecraft with spin axis <0.2° from Sun center; 15 rpm spin rate(12-20 rpm acceptable) (see Sec. 2.b.1).
3. Attitude determination:	Instrument SAS & RAS give spin axis attitude to 1.5 arcsec, roll 3 arcmin (see Sec. 2.b.1).
4. Orbit determination:	Doppler ranging to <10 km in position and <10 m/s in velocity. The orbit determination accuracy needed by the ground station to acquire the spacecraft will be sufficient for the science data analysis.
5. Communication requirements:	Average data rate: ~50 kbps. Required downlink capability to dump 12 Gbits from instrument memory in 48 hours, satisfied by TOTS groundstation at Guam with ~2.25 Mbps downlink and 2 kbps uplink (see Sec. 2.f).
6. Mission lifetime:	2 years nominal, 3 years desired.
7. Launch and/or operational windows:	Launch by end of 1999 highly desirable; by end of 2001 acceptable.
8. Orbital requirements:	Baseline Mission: equatorial, $\lesssim$ 2.5° inclination to skirt SAA, 600±20 km altitude orbit. Minimum Science Mission: 7.5° inclination, 600±20 km altitude.

After the GeDs are cooled to their operating temperature (in ~3 days), **normal science operations** will begin. Science data will be continuously stored in the instrument memory and dumped automatically every orbit to the single Transportable Orbital Tracking Station (TOTS) at Guam. The annual observations of the Crab Nebula require no change from the normal solar-pointing mode.

The required **HESSI launch date and useful mission lifetime** are determined by the timing of the next solar activity maximum. Predictions based on the last two solar cycles indicate that several thousand hard X-ray flares and over 100 γ-ray flares will be detected in a two- or three-year HESSI mission starting at the end of 1999 (Figure 2.a.1). Even a launch as late as the end of 2001 or an unusually early solar maximum would not reduce the predicted number of hard X-ray flares below 1500. Thus, the first of the two MIDEX missions being selected through this AO, with a launch in December 1999, would be ideal for HESSI, with the second mission still acceptable.

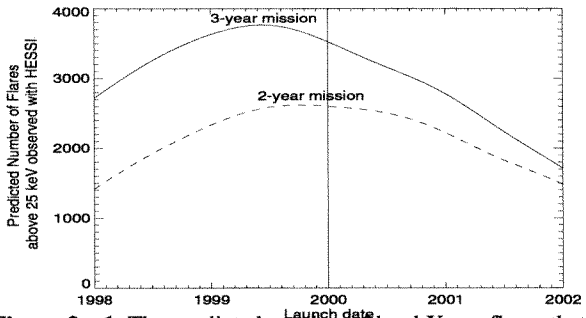

Figure 2.a.1. The predicted number of hard X-ray flares that HESSI will detect in a 2- or 3-year mission versus launch date, based on the X-ray flare rates measured with HXRBS on SMM and BATSE on CGRO over the last two solar cycles (assuming the mean period of 10.6 years for the last seven cycles).

Ground-based observatories are a unique source of the optical and radio data (Table 2.a.2) that are crucial to the successful interpretation of the HESSI data. We have allocated HESSI funds (see Volume III) for the necessary upgrading of hardware at these observatories to provide measurements with adequate temporal resolution, dynamic range, data handling capabilities, etc., for comparison with HESSI's observations. For two facilities that lack long-term support, we will provide the minimal support during the mission to ensure the operation of these critical and unique instruments.

Table 2.a.2. HESSI US Ground-based Program

Filter-based vector magnetograms	MSFC, BBSO
Stokes-polarimeter vector magnetograms	NSO/SP, BBSO
Microwave imaging spectroscopy	OVRO
Optical imaging spectroscopy	BBSO, NSO/SP
Millimeter-wave imaging	BIMA
Full-disk images, magnetograms	NSO/SP,/KP, BBSO
High-resolution imaging	BBSO
Multiband imaging	NSO/SP
Microwave and optical patrols	SOON, RSTN

2.b. INSTRUMENTATION

Table 2.b.1 gives the design heritage for the instrument components. The table in the fold-out gives the basic instrument information requested by the AO.

Table 2.b.1. HESSI Instrument Heritage[1]

Spectrometer	
Germanium Detectors	HIREGS, HEXAGONE balloon
Silicon Detectors	Einstein, ISEE-3, WIND
Detector Electronics	HIREX, HIREGS balloon
Cryostat	HIREGS, HEXAGONE balloon
Mechanical Cooler	ISAMS/UARS
Imaging System	
Grids	HEIDI balloon, Test Grids
Metering Structure	Telescope Demonstration Unit, HEIDI balloon
Solar Aspect System	HEIDI balloon
Roll Angle System	Breadboard
IDPU	FAST SMEX
Spacecraft Interface	FAST SMEX
IGSE	FAST SMEX
Software	FAST SMEX

[1]See acronym list for descriptions.

2.b.1 IMAGING SYSTEM

Imaging Technique. To achieve arcsecond-class imaging at hard X-ray and γ-ray energies, the only viable method within MIDEX constraints is Fourier-transform imaging. We use bi-grid collimators, consisting of a pair of widely separated grids in front of an X-ray/γ-ray detector (Figure 2.b.1). Each grid consists of a planar array of equally-spaced, X-ray-opaque slats separated by transparent slits. If the slits of each pair of grids are parallel to each other and if their pitches (p) are identical, then the transmission through the grid pair depends on the direction of the incident X-rays. For slits and slats of equal width, the transmission is modulated from zero to 50% and back to zero for a change in source angle to collimator axis (orthogonal to the slits) of p/L where L is the separation between grids (see Figure 2.b.1).

The angular resolution is then *p/(2L).*

Equivalently, for a fixed source, the signal can be modulated by moving the collimator, which in our case is achieved by mounting it on a rotating spacecraft. The detector records the arrival time and energy of individual photons, allowing the modulated counting rate to be determined as a function of rotation angle. Note that **no spatial resolution is required and hence the detector can be optimized for the highest sensitivity and energy resolution.**

For a parallel incident beam, the modulated waveform generated by a smoothly rotating spacecraft has a distinctive quasi-triangular shape whose amplitude is proportional to the intensity of the beam and whose phase and frequency depend on the direction of incidence. For complex sources, and over small rotation angles, the amplitude and phase of the waveform provide a direct measurement of a single Fourier component of the angular distribution of the source (e.g., Prince *et al.* 1988). Different Fourier components are measured at different rotation angles and with grids of different pitches.

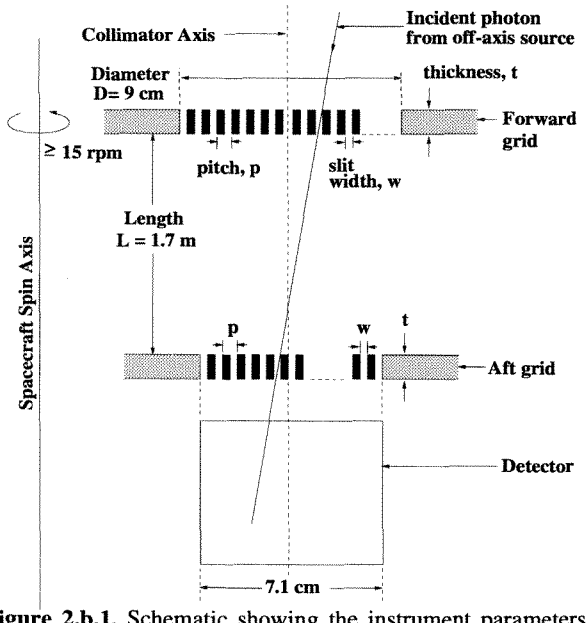

Figure 2.b.1. Schematic showing the instrument parameters that define the imaging capability.

HESSI's Imaging System uses 12 such rotating modulation collimators (RMCs) with L = 1.7 m and grid pitches ranging from 34 μm to 2 mm. This gives angular resolutions that range logarithmically from 2 arcsec to 2 arcmin, to image sources over the range of flare angular scales (Table 2.b.3). Diffuse sources larger than 2 arcmin are not imaged, but full spectroscopic information is obtained. Multiple smaller sources will be imaged regardless of their separation.

In a half rotation (2 s) the 12 RMCs measure amplitudes and phases of ~1800 Fourier components for a typical source location 12 arcmin from the spin axis. This compares with 32 Fourier components for the Yohkoh Hard X-ray Telescope (HXT). Detailed simulations of HESSI's response, using image reconstruction techniques that have decades of heritage from the mathematically equivalent problem in radio interferometry, show that **HESSI can obtain accurate images with a dynamic range (defined as the ratio of the brightest to dimmest feature reliably seen in an image) up to 100:1 (see foldout).**

Although one half rotation is required to measure a full set of Fourier components, the measurement of each component takes a single modulation cycle, which is as short as 1.3 ms for the finest grids. Thus, when count rates are sufficiently high, >1000 c/s per detector, crude images (from about ten Fourier components) can be obtained on timescales of tens of milliseconds. If the source changes on these rapid timescales, space-time confusion can be avoided by using normalization techniques which exploit the fact that the modulation for each RMC occurs at a different rate.

To maximize the range of photon energies that are modulated, the grids are fabricated from high density, high-Z materials (gold or tungsten), and made as thick as possible. Internal shadowing within a single grid limits the FWHM field of view perpendicular to the slats to ~*w/t* (Figure 2.b.1). Thus for HESSI's 1° FWHM field of view, the grid thickness must be less than 57 times the slit width. The angular resolution depends on the slit width, and is thus energy dependent, ranging from 2 arcsec at energies $\lesssim$ 200 keV to 20 arcsec at $\gtrsim$ 1 MeV. The four thickest grids (~2.5 cm) provide $\gtrsim$ 70% modulation at all energies up to 20 MeV.

Matched grid pairs are mounted on stiff, planar grid trays attached to opposite ends of a metering structure (see foldout). A high-resolution, high-bandwidth SAS monitors the imager pointing direction by continuous angular measurements of the solar limbs. A side-looking RAS provides the roll angle information by scanning bright stars. A three-point center mount to the spacecraft supports the Imaging

System above, and completely separate from, the spectrometer.

A detailed error analysis of the imaging performance was carried out and critical engineering requirements (Table 2.b.2) extracted from a preliminary Error Budget. Changing the separation (L) between grids or displacing the grids parallel to the slits has little effect on imaging performance. A relative displacement perpendicular to the slits affects the phase but not the amplitude of modulation. Any such displacement will be accurately monitored by the SAS, and can be fully compensated in the image reconstruction process.

Table 2.b.2. Critical Engineering Requirements for Imaging

Factor	3-σ Requirement	Blurring (arcsec) (FWHM)
Spacecraft Pointing [1]	<0.2°from Sun center	0
Aspect Error In rotating frame In inertial frame	 1.5 arcseconds 3 arcminute in roll	 1.2 0.4
Absolute Solar Aspect[2]	1 arcsecond	0
Grid Imperfections[3]	4.5 microns	0.8
Grid Matching[4,5]	1 part in 3 x 10^4	0.5
Relative Twist[4]	1 arcminute	0.5

[1]Image quality is independent of spacecraft pointing provided Sun center is kept within the 0.2° SAS field of view.
[2]Absolute solar aspect only affects image placement.
[3]Deviation of slit positions from their nominal location within a grid.
[4]Requirement scales linearly with grid pitch--value given is for the finest grids.
[5]Matching of average pitch of the front and rear grid.

The critical alignment requirement is associated with the rotation or *twist* of one grid with respect to the other about the line of sight to the source. A relative twist of p/D (D=diameter of grid) reduces the modulated amplitude almost to zero. Thus, the grid pairs must be well aligned in twist throughout the mission. For the finest grids (2 arcsec resolution) a 1-arcmin alignment is needed. **Thus, HESSI can achieve arcsec-quality images with an instrument having only arcmin alignment requirements.**

It should be noted that Fourier-transform imaging is a relatively "forgiving" process in that moderate alignment errors, even larger than the 3-σ numbers in the error budget, generally only reduce the sensitivity of specific-subcollimators and do not reduce the angular resolution. In-flight knowledge of these errors can be derived from the internal redundancy of the X-ray and SAS data, and applied to the collimator amplitudes and phases to recover most of the nominal telescope performance.

In practical terms, both Yohkoh HXT and SMM HXIS have been coaligned to arcsecond precision using similar technology (Wülser *et al.* 1995; van Beek *et al.* 1980). Compared to both of these instruments, HESSI has the additional advantage that each RMC measures many Fourier components, so that the system is internally self-calibrating in many respects using post-launch data.

Table 2.b.3. Grid parameters

Grid No.	Resolution (arcsec)	Pitch (mm)	Slit Width (mm)	Slat Width (mm)	Thickness (mm)	FOV (deg)	Fabrication Technique	Fabricator
Baseline Mission								
1	2.1 & 4.2	0.070	0.020	0.050	1.1	1.0	Stacking	Delft
2	2.1 & 4.2	0.070	0.020	0.050	1.1	1.0	Stacking	Delft
3	2.9 & 6.1	0.096	0.027	0.069	1.6	1.0	Stacking	Delft
4	6.1	0.101	0.051	0.050	2.8	1.0	Stacking	Delft
5	8.9	0.146	0.088	0.058	5.0	1.0	Stacking	Delft
6	12.9	0.212	0.127	0.085	7.3	1.0	Stacking	Delft
7	18.7	0.308	0.185	0.123	10.6	1.0	Stacking	Delft
8	27.1	0.446	0.268	0.178	15.3	1.0	Stacking	Delft
9	39.3	0.648	0.389	0.259	22.3	1.0	WEDM	GSFC
10	57.0	0.940	0.564	0.376	25	1.3	WEDM	GSFC
11	82.7	1.363	0.750	0.613	25	1.7	WEDM	GSFC
12	120	1.978	1.088	0.890	25	2.5	WEDM	GSFC
Minimum Science Mission								
1	2.9	0.048	0.029	0.019	0.03	44	Gold mask	JPL
2	4.2	0.070	0.042	0.028	0.04	46	Gold mask	JPL
3	6.1	0.101	0.051	0.050	1.0	3.5	Stacking	Delft
4	12.9	0.212	0.127	0.085	1.0	7.2	Stacking	Delft
5	27.1	0.446	0.268	0.178	1.0	15	Stacking	Delft
6	57.0	0.940	0.750	0.190	25	1.7	WEDM	GSFC
7	120.0	1.978	1.088	0.890	25	2.5	WEDM	GSFC

Grids. The grid parameters required for the Baseline and Minimum Science Missions are given in Table 2.b.3. The bottom grids will be 7.1 cm in diameter to match the GeD diameter, and the top grids will be 9 cm in diameter to ensure that the full detector area is utilized for sources up to 0.3° off axis.

Since writing the Step-One proposal, significant progress has been made in the development of the grids, and their integration and testing. We have characterized the test grids using the GSFC Optical Grid Characterization Facility (OGCF) and subjected some of them to thermal cycling and launch-level vibration loads. As a result of these tests, we have established that **all of the grids for the Baseline and Minimum Science Missions can be made now and these grids will meet all the science objectives in the Step-One proposal.** Furthermore, **the selected fabricators have commit-**

ted to meeting the delivery schedule for the first MIDEX.

The coarsest grids (#9 through 12 in Table 2.b.3) are made by wire electric discharge machining (WEDM) of solid discs of a tungsten-nickel-iron alloy (92.5% tungsten). This technique was successfully used to make the HEIDI flight grids with similar dimensions.

Grids #1 through 8 are made by stacking tungsten blades with stainless-steel spacers in a precisely machined Invar reference frame, a technique developed and patented by Co-I, Professor Frank van Beek of Delft University of Technology. **A full-sized 100 μm pitch grid (see foldout) was built at Delft, optically characterized, and vibration and thermally tested at GSFC. It meets all requirements for Grid #4 (6-arcsec from 2 to >500 keV).**

For the finest three grids, Grids #1 - 3, we will use the same Delft stacking technique with a minimum slat width of 50 μm. The required resolution of 2.1 arcsec is achieved by using a slit width of 20-μm and a pitch of 70 μm. The increased slat-to-slit ratio results in a decrease in sensitivity but this can be partially offset by the simultaneous use of this grid configuration for two angular resolutions, using both the first and second harmonics of the modulation profile. This dual use has been previously implemented for the hard X-ray imagers on YOHKOH and Hinotori. **Delft has provided a test grid (see foldout) with 70-μm pitch and 20-μm slit width with the dimensional accuracy and stability needed for Grids #1, 2, and 3.** These grids will provide imaging over the full energy range from 2 keV to >200 keV.

For the Minimum Science Mission, cost-effective performance can be obtained by using two sets of grids, based on the already demonstrated photo-etched gold X-ray mask used in the LIGA process (discussed below). Three full-size, 25-μm thick gold grids with the finest, 34-μm pitch have been made (see foldout). These are supported on a 200-μm thick Si substrate with a pattern of holes in it to allow low energy (to ~2 keV) X-rays to pass through. These grids meet all the dimensional requirements of the MSM, but image only up to ~40 keV.

A consortium of JPL, Sandia Labs, and UCB has been developing fine grids using the LIGA process. A grid pattern exposure is made in acrylic sheet using a synchrotron X-ray beam through a thin gold photo-etched mask. The exposed areas are dissolved away to form an accurate acrylic grid mold, which is filled with gold by electroplating. These grids offer enhanced effective area by a factor of four at the highest angular resolution.

Impressive strides have been made in the past year. **LIGA test grids (see foldout) have been made that meet all the dimensional requirements of the finest grids (34-μm pitch, 20-μm slit width)** except that they are $\gtrsim 400$ μm thick and the acrylic mold material is left in the slits for structural stability. The energy range for imaging with these LIGA grids is ~10 to 200 keV. Thicker grids are now being made to allow imaging to higher energies.

Development efforts for LIGA (and other grid techniques at Artep, Inc., TRW, Mega Engineering, Ultramet, and GSFC) are continuing under Advanced Technology and SBIR funding. A final decision on these enhanced grids will be made during the definition phase.

Metering Structure and Grid Trays

The critical alignment requirement for the metering structure is to maintain the relative twist of the finest grid pair to within one arcminute (see Table 2.b.2). **The proposed metering structure is based on the Telescope Demonstration Unit (TDU) built and tested at GSFC over the last year** (see photograph on foldout). The TDU's on-orbit alignment performance was simulated using SINDA thermal models and NASTRAN structural models. **The results of this analysis and the TDU thermal and vibration tests demonstrate that the proposed design satisfies all the mission requirements.** The TDU consists of 0.81-mm thick aluminum sheet rolled and riveted to three structural rings and nine longerons. The grid trays are machined plates with integral stiffeners. A GSFC study of a composite metering structure showed that an aluminum structure will meet requirements at lower cost and program risk.

To maintain alignment following thermal and vibrational stresses, flexural elements are used to mount the grids to the grid trays and the telescope tube to the spacecraft. This approach was demonstrated with the TDU and used successfully by Co-I van Beek, in the Hard X-ray Imaging Spectrometer (HXIS) on SMM, where the alignment requirements were significantly more stringent. The fine grids will be precision aligned by elastic deflection of these flexure elements.

Thermal blankets, coatings, and 12 watts of heater power are used to achieve a tray-to-tray difference of <3° C. Ten layers of Multi-Layer Insulation (MLI) are used, which still allows imaging down to 2 keV.

Twist Monitoring System (TMS)

Critical twist alignment will be monitored from initial assembly up to launch by the non-intrusive technique illustrated in Figure 2.b.2. This was used successfully by Co-I van Beek to monitor the alignment of the X-ray collimators on the HXIS. The basic technique has been demonstrated at GSFC for digital readout by using a lens-less CCD camera to determine the relative location of diffraction rings from the two alternately illuminated pin-hole sources. An easily measurable 1-μm change in the relative position of the diffraction patterns from the two pinhole/annulus combinations is produced by a 6-arcsec change in twist of one grid with respect to the other.

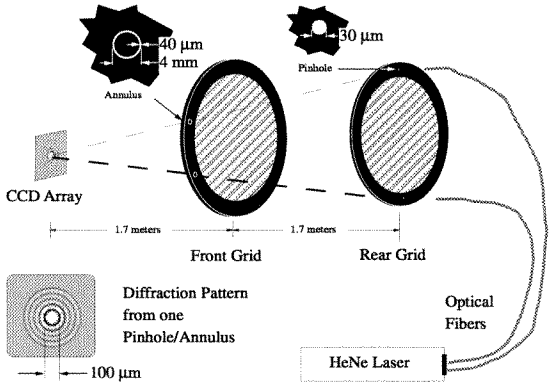

Figure 2.b.2. Pre-flight twist monitoring system

Solar Aspect System (SAS)

The SAS provides (1) high-resolution, high-bandwidth aspect information for image reconstruction, (2) real-time aspect error signals for spacecraft pointing, (3) monitoring of the relative twist of the two grid trays, and (4) full-Sun white-light images for coalignment with ground-based imaging.

The SAS is similar to one flown on HEIDI, which demonstrated 0.5-arcsec performance at balloon altitudes. It consists of three identical lens-filter assemblies mounted on the forward grid tray, which form full-Sun images on three 2048×13-μm linear diode arrays mounted on the rear grid tray (see foldout and Fig 2.b.3). Simultaneous exposures of three chords of the focused solar images are made every 10 ms by each of the arrays. The IDPU uses a digital filter and threshold algorithm to select four pixels across each solar limb for inclusion in the telemetry. With the digitalized pixel outputs, six precise locations of the solar limb are obtained on the ground by interpolation, locating Sun center to 1.5 arcsec. To obtain the six limb crossings, the spacecraft is required to point within ~0.2° of Sun center.

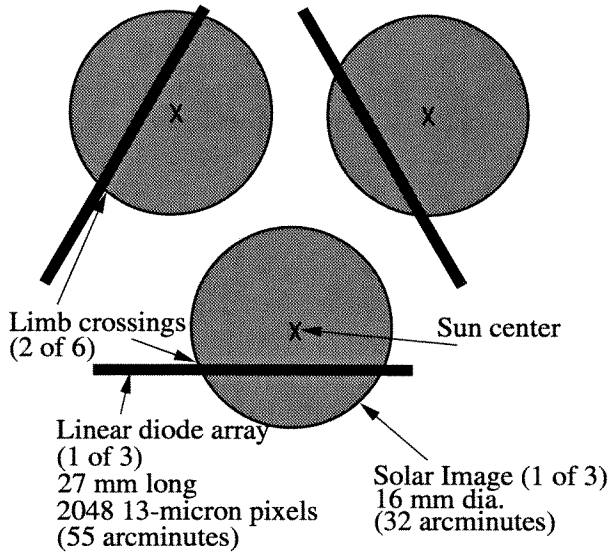

Figure 2.b.3. Schematic illustrating the SAS. The three linear diode arrays and the solar images formed by the three lenses are shown in the image plane, for a pointing offset of 12-arcsec from Sun-center.

Knowledge of the location of the lens' nodal points and the diode arrays on their respective grid trays within several microns is sufficient for subarcsecond aspect performance. Distortions, displacements, and alignment of the metering structure are unimportant since the resulting effects on the end trays are common to both the grids and the SAS components.

The IDPU threshold algorithm also provides error signals with ≲10 arcsec precision in real time to the ACS for spacecraft pointing. Use of the SAS for both imaging and pointing avoids problems of coalignment. Redundancy is provided by the use of three rather than two SASs. For the SAS's use as a solar acquisition sensor, detection of a single limb is sufficient, resulting in an effective radial field of view of 42 arcmin.

Although the aspect solution itself is independent of twist, the internal consistency of each solution provides a continuous, highly sensitive measure of the relative twist of the upper and lower grid trays during flight. Since

SAS lenses are well separated from one another, small twists of the front tray with respect to the rear tray result in characteristically divergent solutions (whose mean, however, is independent of twist). The SAS aspect requirement of 1.5 arcsec corresponds to a sensitivity to relative twist of 0.4 arcmin. During the prelaunch coalignment test indicated in Fig. 2.d.1, this SAS twist measurement is calibrated against that provided by the TMS discussed above.

The digitized output of every pixel of the SAS can be stored in memory to provide a full-Sun white-light image. Simulations show that 5-arcsecond resolution can be achieved. Such data will be used for sensor calibration, but will also show sunspots quite clearly. Although HESSI's X-ray images are absolutely located with respect to Sun center to arcsec accuracy, the sunspot images enable direct coalignment of X-ray images to ground-based optical images, a capability found useful by Yohkoh.

Roll Angle System (RAS)

For image reconstruction on the ground (no impact on realtime spacecraft operations), knowledge of relative roll is required to 3 arcmin (3-σ). Errors in knowledge of the alignment between grid orientations and the spacecraft-mounted RAS have no effect on image quality and only change image placement by up to 0.3 arcsec for a 1-arcmin alignment error. Calculations have shown that the external and internal sources of torque are sufficiently weak that they can be neglected over timescales of a few minutes, so that the required information can be obtained with a star scanner that samples the roll orientation at least once per rotation. Parameterized equations describing rigid-body rotation of the spacecraft then allow the roll orientation to be interpolated at intermediate times with the required accuracy.

The RAS consists of a 2048-element linear photodiode array and electronics (nearly identical to those of the SAS), behind a f/1.0, 50 mm 'camera' lens and sunshade with a $\pm 15^\circ$ field of view which sweeps a 30° band across the sky orthogonal to the spin axis. As the spacecraft rotates, each detected star generates a brief spike in the output of one or two pixels, whose timing defines the roll orientation. The pixel number and pulse amplitude for these spikes are recorded every 2 ms. For +2 magnitude stars, the detection signal-to-noise is 15:1. Even allowing for Earth occultation and the fraction of a second recovery from anticipated Earthshine saturation, at least one such star will be detected each rotation throughout the mission. Multiple measurements averaged over a minute allow the roll angle to be determined to 2.7 arcmin (3σ). More typically, more than seven such stars will be detected per rotation to provide additional performance margin.

2.b.2. SPECTROMETER

The spectrometer consists of the GeDs and SiDs, front-end electronics, the cryostat, and cryocooler. **We emphasize here that all aspects of the spectrometer required for the Baseline and Minimum Science Missions have already been developed.**

Germanium detectors were chosen because they can cover the entire hard X-ray to γ-ray line energy range (10 keV to 20 MeV) with the highest spectral resolution of any presently available detectors. They have been flown previously on the HEAO-3, Mars Observer, and Wind spacecraft (GeD designed and fabricated by UCB/LBNL). Segmented GeDs of the type appropriate for HESSI were developed by UCB (Luke 1984), and over twenty have been successfully flown on HEXAGONE, HIREGS, and other balloon payloads (Smith *et al.* 1993, 1995; Pelling *et al.* 1992, Feffer *et al.* 1993) since 1988. These segmented GeDs have proven to be very robust; the first ones fabricated and flown are still operating with no detector failures to date.

Functional description

The GeD inner electrode is divided into three contacts that collect charge from three electrically independent detector segments defined by the electric field pattern (see foldout). This provides the equivalent of a thin planar GeD in front of a thick coaxial GeD, plus a bottom "guard-ring". The top and curved outer surfaces are implanted with a thin (~0.3-μm) boron layer to provide a surface transparent to >10 keV X-rays.

The front segment thickness is chosen to stop photons of energies from ~10 to ~150 keV, where photoelectric absorption dominates, while minimizing the active volume for background. Front-incident photons that Compton-scatter, and background photons or particles entering from the rear, are rejected by anticoincidence with the rear segment. In addition, a passive, graded-Z (Pb, Cu, Sn) shield around the curved outer surface of the front segment absorbs hard X-rays incident from the side, so the front segment has the low background of a

phoswich-type scintillation detector.

Photons from 150 keV to 20 MeV in energy, including nuclear γ-ray lines, are detected primarily in the thick rear segment. Some also stop in the front segment, some deposit their energy in both the front and rear segments, and some deposit their energy in two or more detectors. These modes also contribute to the total efficiency and are identified accordingly.

The large flares that produce significant γ-ray line fluxes usually produce intense ≲ 150 keV hard X-ray fluxes. Segmentation allows the front segment to absorb these low energy fluxes, so the rear segment will always be counting at moderate rates to provide γ-ray line measurements with optimal spectral resolution and efficiency (low dead time). The front segment electronics are designed to provide high rate (up to 5×10^5 c/s) hard X-ray imaging in broad energy bands.

Hard X-ray and γ-ray photons from (non-solar) sources can penetrate the thin aluminum cryostat wall from the side and be detected by the GeD rear segments.

Radiation effects

Reverse electrode (n-type) coaxial GeDs were chosen because of their relative immunity to radiation damage. The Baseline Mission's 600-km equatorial orbit was chosen to skirt the intense trapped radiation from the SAA, while all solar flare energetic particles and primary cosmic rays below ~10 GeV are excluded by the Earth's magnetic field. The low cumulative fluence (6×10^6 cm^{-2} in >30 MeV protons for a three-year mission lifetime near solar maximum) completely eliminates resolution degradation even with no shielding.

The Minimum Science Mission orbit, 600 km circular at 7.5° inclination, results in a fluence of 5×10^8 cm^{-2} of >30 MeV protons in two years near solar maximum, still below the 10^9 cm^{-2} threshold for significant resolution degradation. Thus, neither shielding nor detector annealing (which can reverse the radiation damage effects but entails complexity and risk) is required. Radiation damage decreases with lower temperature, but increases with warmups above ~85K, or detector high voltage cycling. The cryostat is designed with large margins to ensure that temperatures below 85K can be maintained once operation begins, and the High Voltage Power Supplies (HVPS) are designed to be on at all times after turn-on.

GeDs and Modules. HESSI will use the largest, readily available, hyperpure (n-type) coaxial germanium material (7.1-cm in diameter × 8.5-cm long). The GeDs are segmented into 1.5-cm front and 6.5-cm rear detectors plus a guard ring (see foldout).

The most common failure mode for GeDs is from contamination of the intrinsic (flat rear) surface, leading to increased surface leakage current and noise. For planar GeDs and SiDs, guard rings are often used to isolate and drain off the leakage current of the intrinsic surfaces. UCB has recently developed guard-ring coaxial GeDs, using our proven segmentation technique (Luke, 1984). Tests with a prototype coaxial guard ring GeD showed that surface leakage currents of one nanoamp (~ten times higher than usable for non-guard-ring GeDs) resulted in no degradation, and currents of 10 nanoamps resulted in a few hundred eV broadening in resolution, which is still acceptable. **This increased resistance to contamination, by a factor of ~10^2, allows the use of a single vacuum enclosure for all 12 GeDs** instead of the more complex and expensive hermetic encapsulation of individual detectors.

The mechanical design of the GeDs and their mounting module (see foldout) is identical to that for the HEXAGONE and HIREGS instruments, which have survived many balloon flights and recoveries. The use of teflon and gold foil to accommodate surface irregularities between detector and mounting hardware provides a rugged module which has been successfully vibration-tested and is fully capable of surviving a Med-Lite launch.

Silicon detectors (SiD)

The SiDs are standard Si(Li) guard-ring detectors of ~1 cm^2 area and ~3 mm thick. Passivated surfaces make them highly insensitive to contamination in the ambient environment. Many such SiDs have been fabricated by UCB and successfully flown on previous NASA missions. The grounded guard-ring is used not only for shunting large surface currents to ground but also for detector retention and cooling. The detector mount is fabricated from low-Z materials, with a beryllium foil entrance window.

Recently UCB has been developing silicon drift chambers which can provide spectral resolution and energy range similar to Si(Li) detectors, but operating at room temperature. If this development progresses sufficiently rapidly, they may replace the Si(Li) detectors. This would significantly simplify the cryostat wir-

ing, and lower the cooling load.

GeD and SiD front-end electronics

The input FETs are mounted close to the GeD, as in HEXAGONE and HIREGS, to provide a high level of noise immunity. The FETs are thermally isolated from the detector, and thermally connected to the cryostat thermal shield to keep them at optimum operating temperatures of ~140K (not critical). Hybrid Charge Sensitive preAmps (CSAs), two per GeD, and individual HVPSs for each GeD are mounted outside on the cryostat side wall (see foldout). All high voltage leads are fully shielded from external surfaces to avoid microphonic noise pickup. Crosstalk noise is minimized by using separate photolithographically-etched signal cables for each detector channel. Ground loops are minimized by a star ground at the vacuum shell of the cryostat.

The FET is an integral part of each SiD package. Each SiD is biased at ~300V by an independently programmable regulator from a common high-voltage supply.

Cryostat

The GeDs in their non-hermetic detector modules are mounted in the cryostat on an aluminum coldplate, in a configuration very similar to the HIREGS instrument. A shield over the front of the coldplate encloses the GeDs and isolates them from IR radiation and from contamination sources in other parts of the cryostat. A simple labyrinth seal prevents contamination inside the IR/contamination shield from reaching unacceptable levels over the life of the mission. The shielded GeD assembly is surrounded by a thermal shield (at ~140K), then blanketed with MLI.

The SiDs and their FETs are mounted on the thermal shield, along with thermal straps from the GeD FETs. The thermal shield provides a stage at which the power of all the detector FETs may be efficiently dissipated, and attenuates the parasitic thermal load on the coldplate. The shield and coldplate are supported inside the cryostat vacuum shell by a set of six fiberglass struts. The top cylinder and bottom plate of the cryostat are removable for access to the front and back of the coldplate.

The body of the cryocooler, vacuum manifold, housekeeping connectors, and a liquid nitrogen feed connection are also mounted on the vacuum shell together with the CSAs and HVPSs. The front plate of the cryostat has beryllium windows in front of each detector, as in the HEXAGONE instrument, allowing filters to be added for optimizing the response across the energy spectrum. The curved side wall of the cryostat near the GeDs are ribbed thin-wall aluminum to provide a low energy threshold for X-ray/γ-ray sources viewed out the side.

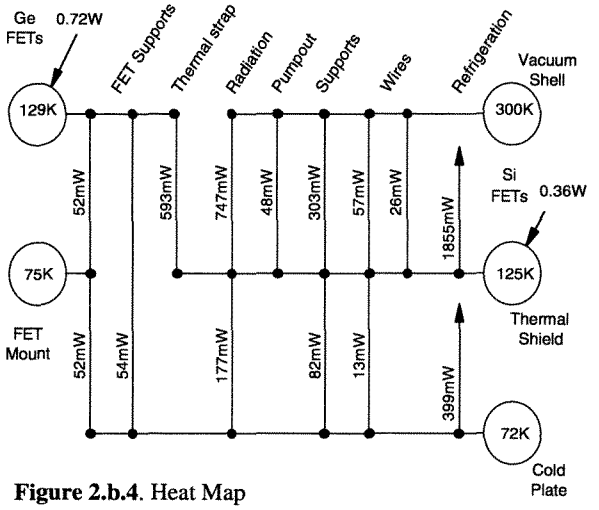

Figure 2.b.4. Heat Map

Cryocoolers

The coldplate and thermal shield are cooled on-orbit by mechanical refrigerators (cryocoolers), but are kept cold during ground operations by a simple liquid nitrogen cooling loop. On-orbit either two small single-stage cryocoolers or a single two-stage cryocooler will be used to maintain the coldplate below 85K and the thermal shield at ~140K. The thermal shield is loaded in roughly equal proportions by parasitics and FET dissipation.

Three different long-life cryocoolers, from Ball, Matra/Marconi and TRW, have been extensively evaluated for this application. All are designed with moving components that are suspended on flexure springs and are precisely aligned to prevent any contact throughout the lifetime of the mission. They are available with a nominal 50,000 hour (~5-year) lifetime, which is set mainly by the electronics. Multi-year lifetime has been demonstrated in space flight on the European ERS-1 and NASA's UARS missions, and in ground testing at ESA.

A detailed, thermal model of the cryostat (Figure 2.b.4), taking into account the wiring, MLI blankets, support structure, and cryocooler characteristics, was used to study design options, and to evaluate the performance of the available cryocoolers. Each of the three cryocooler options is capable of maintaining the

coldplate below 85K, with better than 5K margin.

An important consideration is noise in the GeDs from microphonics and electrical pickup from the mechanical coolers. The cryocoolers all have carefully balanced components to minimize vibration. Active vibration damping (using force transducers or accelerometers as sensors and then tuning the motor signals to damp) is a standard feature of the electronics from each of the cryocooler manufacturers. In the past two years we have conducted tests with three different mechanical coolers (TRW pulse tube, Lockheed/Lucas and Ball Stirling cycle) designed for long-life space missions, using a UCB balloon payload coaxial GeD in standard UCB module. These tests were done with the coolers running open-loop **without** active vibration damping. **In all three tests microphonic noise was found to be negligible**. For two of the coolers some resolution broadening (from ~2.5 keV to ~3 keV FWHM) was observed due to electrical pickup from the cooler electronics. However, for HESSI the cryocooler and cryocooler electronics will be electrically isolated from the cryostat and grounded back at the power supply. This configuration was tested with the third cooler and **the GeD showed no measurable (<0.1 keV) difference in the energy resolution or noise background with the cryocooler on or off.**

2.b.3. INSTRUMENT ELECTRONICS

System Overview. Figure 2.b.5 shows the overall electrical system block diagram for the instrument and the spacecraft. Low level detector signals from the CSAs are amplified, processed, and converted to digital by 12 identical analog electronics boards, one for each GeD/SiD combination. The IDPU collects and formats data from the analog system, the SAS, the RAS, and the cooler. Data are stored in the solid-state recorder (SSR). The IDPU also contains the interface to the spacecraft MUE system for receipt of ground and stored commands, exchange of housekeeping and status information, and transmission of data from the SSR during ground contacts.

The IDPU digital electronics is nearly identical to that of FAST. As on FAST, to reduce interfaces, weight, power, and cost, almost all of the electronics is packaged in a single box.

Detector Analog Electronics. Each GeD is biased at between 4 and 5 kV by a separate adjustable HVPS mounted on the cryostat. The design is based on a miniature high reliability Cockroft-Walton stack developed at UCB and has been used on HIREGS and spacecraft experiments. A common 300-volt supply in the IDPU provides the bias voltage for the silicon detectors, with a separately adjustable regulated output for each one.

Photons interacting in a GeD or SiD generate charge pulses, which are collected and amplified by CSAs (Figure 2.b.6). All CSAs will use an advanced 4-terminal FET, developed for UCB with NASA SR&T funds, with 3-4 times the gain and half the capacitance of commercial units. This provides state-of-the-art energy res-

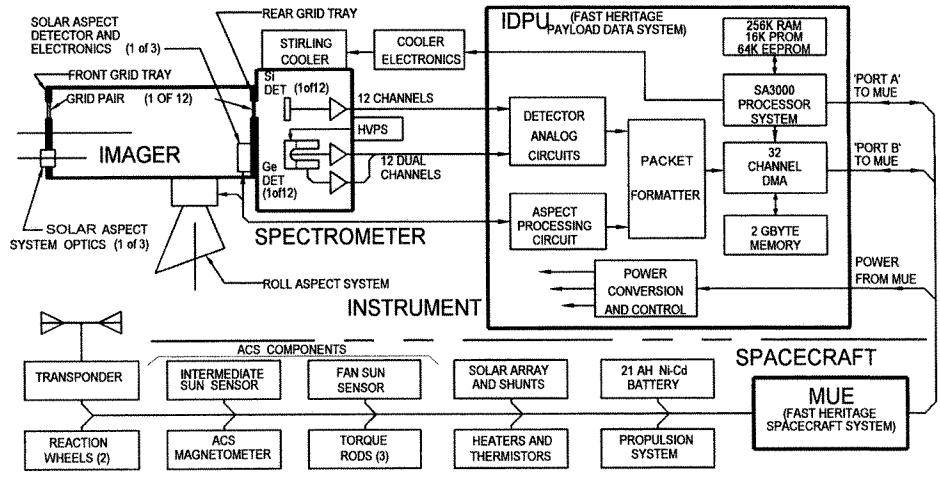

Figure 2.b.5. Instrument and electronics block diagram showing the different elements of the instrument and the connections to IDPU, the MUE, and the spacecraft.

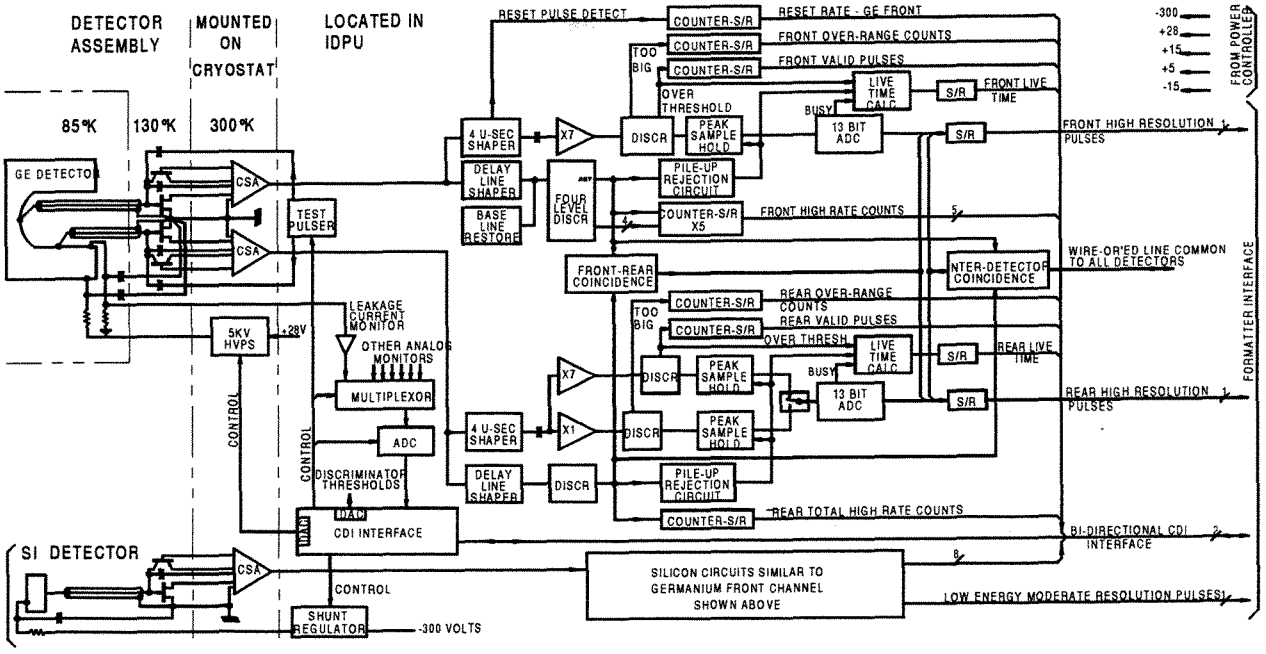

Figure 2.b.6. HESSI front-end block diagram for one detector channel.

olution and high count-rate performance with minimum power consumption. For best noise performance, the input FET is cooled to ~140K, and the rest of each CSA is mounted, on the cryostat near the detector.

A transistor-reset CSA is used to provide the best resolution and high-count rate performance, and to avoid problems associated with pole-zero cancellation. The CSAs will be miniaturized by a commercial firm to chip and wire hybrid circuits from UCB designs. This circuit was developed at UCB for the HIREX balloon instrument, and is now used throughout the nuclear instrumentation industry where the highest performance is needed. The reset pulses are monitored since the rate is a direct measure of the bulk leakage current and thus the health of the GeD. The surface leakage current of the guard rings is also monitored by the IDPU to give another indication of GeD health.

GeD Front Segment. The CSA signal from the front segment of each GeD goes to two parallel signal processing chains on the IDPU analog boards (Figure 2.b.6). The high resolution ("slow") chain consists of a 9-pole quasi-trapezoidal filter amplifier with a peaking time of 4 μsec, a peak stretcher, and a 16-bit successive approximation ADC. Quasi-trapezoidal filtering compensates for ballistic deficit effects of the charge collection in large detectors to maintain good resolution at higher energies ($\gtrsim$1 MeV). The upper 13 bits of the ADC provide 8192 channels of spectral measurements from ~10 keV to 2.7 MeV with ~0.33 keV/channel at rates up to 50,000 c/s. The 1/4 LSB converter gives a differential nonlinearity of <3%.

The high rate ("fast") chain consists of a delay-line shaper generating a triangular pulse of 0.5 μs duration, which is sent to a pileup rejection circuit and a 4-channel stacked discriminator ADC. The short integration time and narrow pulse width provide a count rate capability in excess of 500,000 c/s. At count rates from 10,000 to 500,000 c/s, the accumulated output of these four channels will be sampled at a rate of 16 kHz to provide broad-band ($\Delta E/E \approx 1$) imaging when the slow chain saturates with events. The signal from the LLD of the fast channel is used to detect front-rear and detector-detector coincidences, and for pulse pileup rejection. A live time counter enables deadtime corrections to be made on the ground. At rates >500,000 c/s, the CSA reset rate serves as a measure of the total flux and provides deadtime correction.

GeD Rear Segment. With its larger volume, the GeD rear segment is much more efficient at stopping high energy photons. Therefore, a second low-gain amplifier and peak stretcher (Fig. 2.b.6) is added to extend the energy range to ~20 MeV. The ULD at 2.7 MeV switches the input of the 16-bit ADC to the low gain (high energy) side to provide ~2.4 keV/channel resolution up to 20 MeV, sufficient to resolve the

wider solar γ-ray lines above 2.7 MeV.

Si Detector Electronics. Each SiD CSA feeds dual amplifiers: a slow chain with a 5-pole $\sin^4$ filter with a 4-μsec peaking time which drives an 8-bit flash ADC, and a fast delay line shaper which generates a triangular pulse of 0.5 μsec duration which drives the pile-up rejection circuit and a 4-channel set of stacked discriminators. The slow chain is used for high resolution measurements up to 50,000 cps, while the fast chain gives 4-channel broadband imaging at up to 500,000 cps.

A **calibration pulse generator** injects a precisely generated charge pulse into the front end electronics of the GeDs and SiDs at ~0.3 Hz for detector electronics calibration and monitoring throughout the flight.

Digital System. (see Figure 2.b.5) The **Formatter** (based on FAST) uses a number of Field Programmable Gate Arrays (FPGAs) to perform all high-rate data handling by writing data directly into the SSR using a 32-channel Direct Memory Access (DMA) system. Data from up to 30 sources can be simultaneously formatted into separate CCSDS packets and transferred to the SSR, while data are simultaneously read out to telemetry.

Processor. The IDPU microprocessor system coordinates Formatter activities, allocates space in the SSR, monitors instrument status, formulates housekeeping packets, interfaces with low-rate data sources, and interfaces with the spacecraft MUE 'Port A' for all transactions except high rate telemetry. **It is based on a Sandia SA3300 microprocessor and is identical to the system flown on FAST.** It has bootstrap and baseline code in PROM, with additional code in EEPROM. The processor will have turn-on sequences to configure the instruments, and safing sequences which respond automatically to triggers based on instrument housekeeping.

Solid-State Recorder. The SSR in the IDPU stores data until it can be transmitted. It is capable of random access at 20 Mbits per second. The SSR is sized (2 Gbytes) to hold all the high energy data from the largest solar flare. The recorder will be constructed using the same board layout and chip-stacking system used in FAST, but with higher capacity memory chips.

Data Formatting. Formatting of the data follows that of HIREGS. For each detected photon, the energy (13 or 14 bits for GeDs, 8 bits for SiDs) and time of arrival (to 60 μs) are encoded together with detector identification and coincidence flags into a 24-bit event word. This is stored in the SSR together with SAS and RAS data and housekeeping.

SSR usage is optimized by storing events in a variable format which adapts to the event rate. The main limitation is the orbit-averaged downlink rate. As the SSR approaches full, the processor reduces the input event rate by sub-sampling. This is achieved by collecting enough events from a set of detectors to produce an image, and then disabling input from those detectors for a time interval that depends on how full the SSR is. Events are collected for an integer number of half-spins to achieve full angular coverage. The SiDs start sub-sampling first. At 75% SSR capacity, the GeD front segments start sub-sampling. GeD rear segments produce such a low event rate that they never need to be sub-sampled. When the SSR is nearly full, sub-sampling will reduce the input rate to match the expected downlink rate. Detailed modeling shows that even in the most active times, this scheme is sufficient to keep the SSR from overflowing, with minimum loss of imaging capability and no loss in γ-ray spectroscopy.

The IDPU to MUE interface will be identical to that of FAST. The interface consists of Port B for high speed telemetry transfer from the SSR, and Port A which is used for all other communications. Port A is a redundant bi-directional RS232-like serial interface. The IDPU provides instrument housekeeping packets to the MUE which combines these packets with spacecraft housekeeping packets. The full housekeeping telemetry stream is then returned to the IDPU for storing in the SSR or for immediate transmission. The MUE also has the capability of sending housekeeping directly to the transmitter, bypassing the IDPU. Port B is a simple serial interface with a clock and frame gate provided by the MUE, and a serial data stream provided by the IDPU.

SAS and RAS Electronics. The SAS and the RAS are both based on a Reticon linear charge-coupled photo-diode array, and use virtually identical electronics. Front-end circuits mounted near the sensor consist of a clock generator and drivers, a multiplexor to switch between the video outputs, and a 10-bit high speed ADC with a precision reference. The board also includes a hardware blocker to format the 10-bit values into 16-bit words and a first-in-first-out

(FIFO) memory to buffer data into convenient blocks for serial transmission to the IDPU. The digital circuits are implemented in a single FPGA with a RAM chip used to make the FIFO.

The rest of the electronics (implemented in FPGAs on the Formatter circuit board) consists of hardware circuits to perform data averaging and comparisons for the aspect determination algorithms. The data are used by the IDPU processor to calculate an aspect error signal for the on-board closed-loop ACS.

Selected raw SAS data samples taken near the limbs are stored into the SSR with the instrument data for use in a fine aspect solution on the ground. Time-tagged RAS events, are also stored and telemetered to indicate when bright stars are in the RAS field of view for use in the roll aspect solution on the ground.

Cooler Electronics. The cryocooler electronics (furnished by vendor) provide autonomous startup and shutdown of the cryocoolers, efficient DC-AC power conversion for the linear motors, temperature/stroke control of the compressor pistons, signal conditioning for an accelerometer and two temperature sensors, and vibration control of the compressor and displacer. These will be packaged separately and mounted near the mechanical cooler. A serial interface to the Formatter carries low-rate commands and housekeeping.

Power. The IDPU receives primary 28V power on two switched circuits from the MUE. One of these circuits is used to power the basic processor, Formatter, and SSR, while the second powers the detector electronics and the SAS and RAS. A set of DC-DC converters in the IDPU generates secondary power which is separately current limited and switched to allow individual control of each sub-system. Primary 28V power is supplied directly to the cryocooler from the MUE.

2.c. SPACECRAFT

HESSI is based extensively on the FAST and SWAS spacecraft described in Appendix B of the AO. The basic design is governed by two fundamental requirements: the instrument must point to the Sun and it must spin about the solar-pointed axis. These requirements are most economically accommodated by a Sun-pointed spinning spacecraft (see foldout).

The estimated weight and power for HESSI are 408 kg and 191 watts respectively. This provides margins of 22% in weight and 20% in power based on the AO offered Med-Lite Launch Vehicle and the 240 watts orbit average power capability (AO Page B-4).

Spacecraft Description

Following submission of the Step-One proposal, **the spacecraft concept has been changed to include a mono-propellant hydrazine propulsion system.** For the Step-One proposal, the information provided to us by the MIDEX Office indicated that the Med-Lite launch vehicle could achieve a 600-km altitude equatorial orbit with altitude dispersion of ±10 km. Subsequently, we have learned that the altitude dispersion will be ±350 km (3σ). This error is caused by the pointing uncertainty of the final unguided stage solid Star 37 motor. For circular orbits with altitudes less than 580 km, the spacecraft will re-enter the Earth's atmosphere in less than three years, and above 700 km altitude the instrument's GeDs will be subject to radiation damage from the SAA.

The **propulsion system** consists of three separate modules each containing a 33-cm spherical tank pressurized to 2.41MPa, a 4.5N catalytic thruster, and associated pressure transducers, filters, isolation valves, thermal insulation and heaters. These modules are mounted outboard of the primary structure between the three solar arrays with the center of the tanks in the plane of the spacecraft CG (see foldout). They are structurally, thermally, pneumatically, and functionally independent of each other. This arrangement simplifies spacecraft integration and permits the spacecraft dynamic balance to be independent of the fuel level in each tank. Spacecraft static imbalance has negligible effect on the Sun-pointing performance.

The propellant load of 37.6 kg can correct the worst-case orbit, 250×600 km, to a nominal 600 km circular orbit with a margin of 6.7 kg or 21.7% fuel reserve. Following orbit correction all remaining fuel will be expelled to save the 15 watts of heater power needed to prevent fuel freezing. Final component selection during the definition phase will be based on recent heritage.

The **electrical system** (Fig. 2.b.5) is based on the FAST SMEX architecture described by AO Page B-18, B-19, and Table B-3. The MUE controls the C&DH system, power, ACS electronics, and the propulsion system. It interfaces to the instrument IDPU, which contains the 2-Gbyte solid-state record-

er, data processing and formatting electronics and instrument sensor electronics. About 85% of the existing FAST MUE hardware can be duplicated for HESSI and most of the existing software can also be used. One additional magnetic torquer driver will be added for the third torquer bar and two new cards containing propulsion system valve drivers will be needed. Some of the power relays and wiring will need to be changed to service the larger power needs of HESSI (190 vs. 48 watts). Reaction wheel drive electronics are located in a separate box, offered in Table B-1 of the AO.

The Direct Energy Transfer **power system** is controlled by the MUE. The three identical 2-m^2 solar panels are stowed for launch and are hinge-deployed through 90° so that the plane of the solar cells is perpendicular to the spin axis. The robust hinges and strut locks support the deployed arrays for dynamic balancing in a 1-G environment before launch. The 21-AH NiCd battery is sized for a maximum depth of discharge of only 22%.

Spacecraft Geometric and Thermal Math models were used to analyze the spacecraft thermal environments and define the location of radiators, MLI, and heater power requirements to safely maintain all spacecraft component temperatures within acceptable limits throughout the mission. Except for the propulsion system, all spacecraft components are passively thermally controlled between -15°C and +50°C (battery temp. is 1 to 15°C) without heater power. As noted, 15 W will be required to maintain the propulsion system limits during the orbit adjust. Following fuel expulsion these heaters will be turned off.

Using magnetic torque rods, the FAST-based **ACS** points the spacecraft to within 0.2° of the Sun center, spins it up to 15 rpm, and maintains that rate. A Fan Sun sensor with FAST heritage is used for the initial autonomous Sun-acquisition maneuver. It is substituted for the SWAS digital Sun sensor offered in the AO since it is better suited to a spinning spacecraft. Since the cost of these sensors are comparable, it is assumed that the instrument will not be charged for this exchange. This sensor, together with the 12° FOV Intermediate Sun Sensor (ISS), provide the control signals necessary to ensure Sun acquisition from any attitude until the Instrument SAS becomes the primary sensor for pitch and yaw pointing signals during the science mode. The ISS cost is charged to the Instrument. A FAST high-fidelity simulation reconfigured with HESSI payload parameters has demonstrated the adequacy of the three 130 amp-m^2 torque rods in an equatorial orbit.

Both the instrument and the spacecraft will operate autonomously for days at a time. With the spacecraft spinning at 15 rpm and pointing at the Sun, HESSI is passively spin stabilized because the spin/transverse mass moment of inertia ratio is greater than 1.0 (1.08).

The **primary structure** is traditional aluminum construction based on the flight- proven 6019 Delta launch vehicle payload attachment fitting. The ratio of the structure to the total lift-off mass is 13%. Although this is less than that recommended in the AO, Appendix B-3-A, we believe that this is reasonable. The structure is simple, the concept has heritage, and a detailed finite element model shows that the fundamental resonance is above 25 Hz. The Delta launched COBE spacecraft, designed and built at GSFC, had a mass ratio of less than 10%. The open design permits ample radiator area for heat rejection and enables easy access to subsystems. All major subsystems are attached to the middle deck allowing the Spectrometer to have an open radial field of view for cosmic sources.

The Spectrometer is installed from beneath the spacecraft and bolted at three locations to the base of the primary structure. The Imager is installed from above and bolted to mounts which are located on the top deck. The Spectrometer and Imager are not structurally connected to each other.

Spacecraft dynamic balance, which affects the 0.2° instrument pointing accuracy, is a critical issue. Recent experience with the Wind spacecraft shows that spinning spacecraft can be balanced on the ground to within 0.1°, and maintained through launch and orbit without an onboard balance adjustment. During the definition phase, studies of the HESSI dynamic imbalance sensitivity will continue. Until then, two AO offered reaction wheels have been included in the spacecraft, to retain the option for on-orbit dynamic balance. These are capable of dynamically balancing HESSI from 0.5° to less than 0.1°.

The HESSI **RF system** uses the 5 watt S-band transponder, two omni antennas and a combiner assembly offered in the AO page B-7. Link analysis indicates a 3-dB margin is

maintained over 85% spherical coverage for downlink and 95% spherical coverage for uplink. This analysis assumes a downlink rate of 2.25 Mbits/s (the same as for FAST) at the maximum slant range of 2675 km to a TOTS 8-m antenna with a bit error rate $<1\times10^{-5}$. A detailed analysis of the ground station contact time with a station at Guam indicates that 12 Gbits of data can be downlinked within any 48-hour period to meet the science requirement for downlink data volume. The cost of transporting the TOTS to and from Guam is included in this proposal, while less expensive CNES, ESA, or Brazilian alternatives are being explored.

Spacecraft Resources

The resources needed for the HESSI mission are summarized in the table on the foldout. Compliance with the AO resources described in Section B-3 are identified and the rationale for deviations are discussed in Section 2.c.1.

Instrument Accommodations

1. Preferred Launch Orientation. The spacecraft spin axis and instrument centerline are co-aligned with the launch axis. This vertical orientation of instrument and spacecraft makes best use of the fairing volume and minimizes bending loads in the Imager.

2. Instrument Location Constraints. The forward looking Imager and Spectrometer occupy the center regions of the spacecraft. Each imager grid pair and the SAS optics need a 1° axial FOV. The Spectrometer must be mounted directly behind the Imager to detect the collimated photons. The GeDs have a secondary field of view which is radially outward for observation of "all sky" cosmic events. The cooler radiator needs a clear view of space for heat rejection. The Roll Angle Sensor (RAS) requires a ±15° FOV with optical axis at right angles to the spin axis. The instrument and spacecraft boxes are placed in a symmetric pattern for balance and heat rejection.

3. Alignment to Axis. The imager telescope centerline must be aligned to within 0.2° of the spacecraft spin axis. The spectrometer must be aligned to the Imager grids to within 1 mm. The RAS optical axis must be known to within 3 arcmin.

4. Baffling or Other Protection. None.

5. Thermal Environment/Temperature Limits. The operational limits of the instrument electronics is -10° to 40°C. Survival limits are -30° to 50°C. The front and rear grids must be kept within 3°C of each other. Thermal analysis has shown that this may be achieved by thermal blankets, and thermostatically controlled (12 W) heaters. The hydrazine thruster limits of +10 to +40°C operational, +8 to +50°C survival to prevent fuel freezing, are maintained using thermal blankets and (15 W) heaters.

6. Data Processing. All on board instrument data processing is performed by the instrument IDPU. Ground data processing requirements are described in the Step-One proposal and in Section 2-f.

7. Telemetry. The HESSI instrument places no unusual telemetry collection requirements on the spacecraft. Only a limited number of temperatures, voltages and currents need to be monitored. The sample rate, time tagging, and format are not critical and are well within MUE capabilities.

8. Commands. Mission operations will be mostly autonomous. HESSI will occasionally need either real-time execution of uplinked commands or storage of commands for execution at a pre-determined Mission Elapsed Time (MET). These command loads will typically be 1 to 2 kilobytes, and will be used mainly for instrument control. Execution of the stored commands needs to be within 100 ms of the on-board MET. Much less than one command load per day is projected for normal operations. These needs are easily met by the MUE and ground system.

9. Timing (clocks). The HESSI instrument will utilize the MET information and the 1 Hz clock from the MUE. The HESSI required MET resolution of 10 ms and on-board absolute time accuracy of 5 s are well within the MUE capabilities. The absolute time for data analysis will be determined to <10 ms on the ground by cross-calibrating the clock in the telemetry with a clock locked to UT on each ground-station pass. The TOTS time capture unit can achieve this cross-calibration to within 1-2 ms.

10. Environmental Sensitivities. HESSI has no specific environmental sensitivities relating to electrical, magnetic fields, cleanliness, or contamination. The standard MIDEX class 300,000 clean room is adequate for payload integration. The detectors and cryostat will be assembled and closed in the UCB clean facilities prior to delivery.

11. Data Collection and Storage. All science data is collected by and stored in the in-

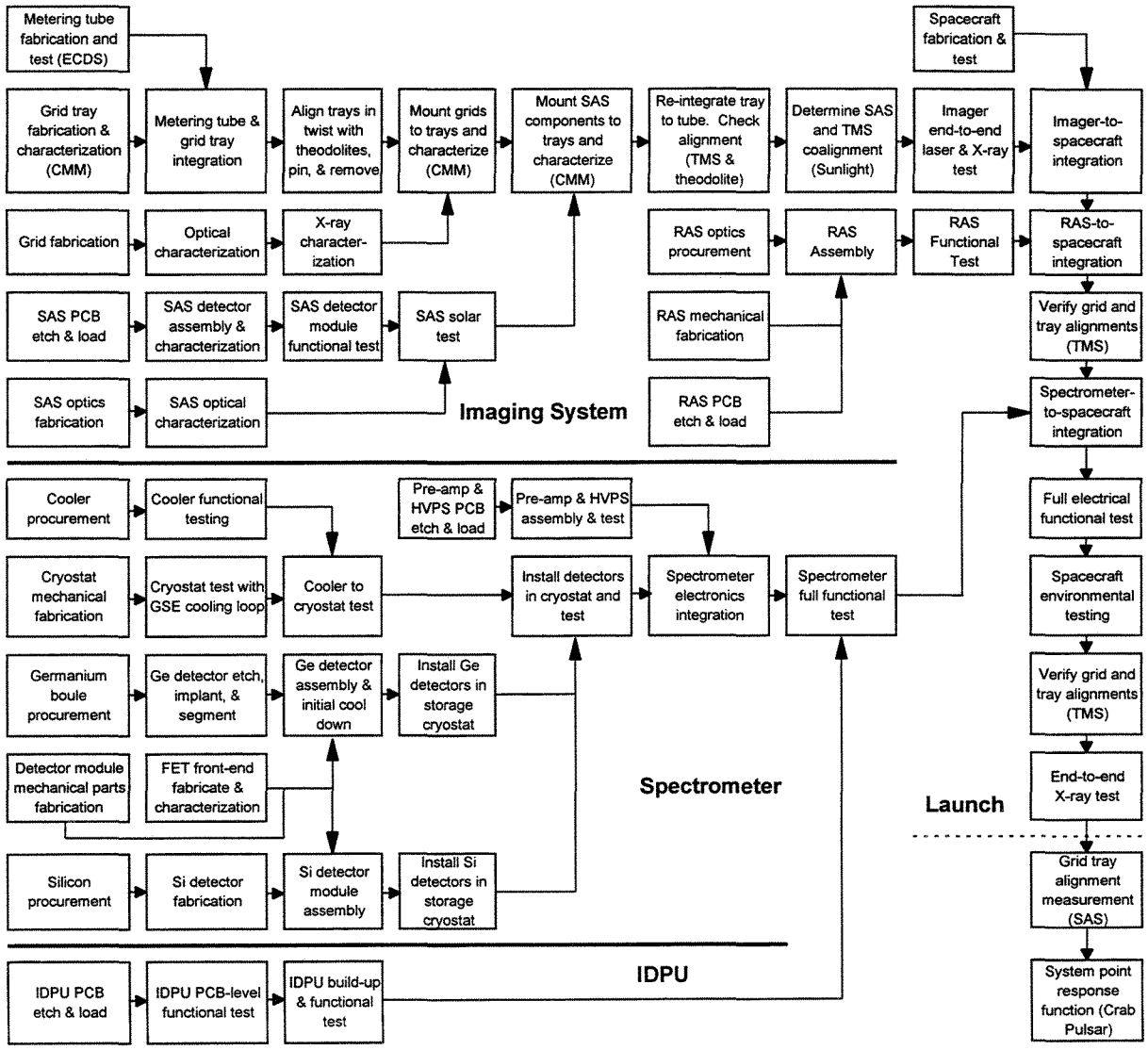

Figure 2.d.1. Manufacturing, Integration, and Test Flow Diagram.

strument IDPU, so C&DH based data storage is not needed. (See RF system discussion in previous section.) Section 2.e describes mission operations in greater detail.

12. Required U.S. Government Support. GSFC is a partner in the development of the HESSI instrument. A full explanation of GSFC roles and obligations are provided in the separate Management Plan (Volume II).

2.d. MANUFACTURING, INTEGRATION and TEST (MI&T) PLANS

Figure 2.d.1 shows the manufacturing, integration, and test flow for the HESSI payload and Figure 2.d.2 gives the schedule.

Electronics MI&T

HESSI electronics manufacturing will be done at the UCB using processes and procedures developed and used on earlier programs including FAST, XDL, and EUVE. In-house fabrication will be done in the UCB/SSL electronics fabrication area using the same personnel as on those programs.

Printed circuit board test coupons will be evaluated by GSFC Code 300 in parallel with the board loading.Boards will be checked out on test beds prior to integration into higher assemblies. All manufacturing, test, and if necessary, rework or repair activities will be recorded in chronological order on an individual Certification Log (manufacturing traveller).

Fully functionally tested boards will be assembled into the following subsystems: 1) IDPU (both GeD/SiD analog and IDPU digital), 2) RAS, 3) SAS detector modules,

Figure 2.d.2. Schedule Summary.

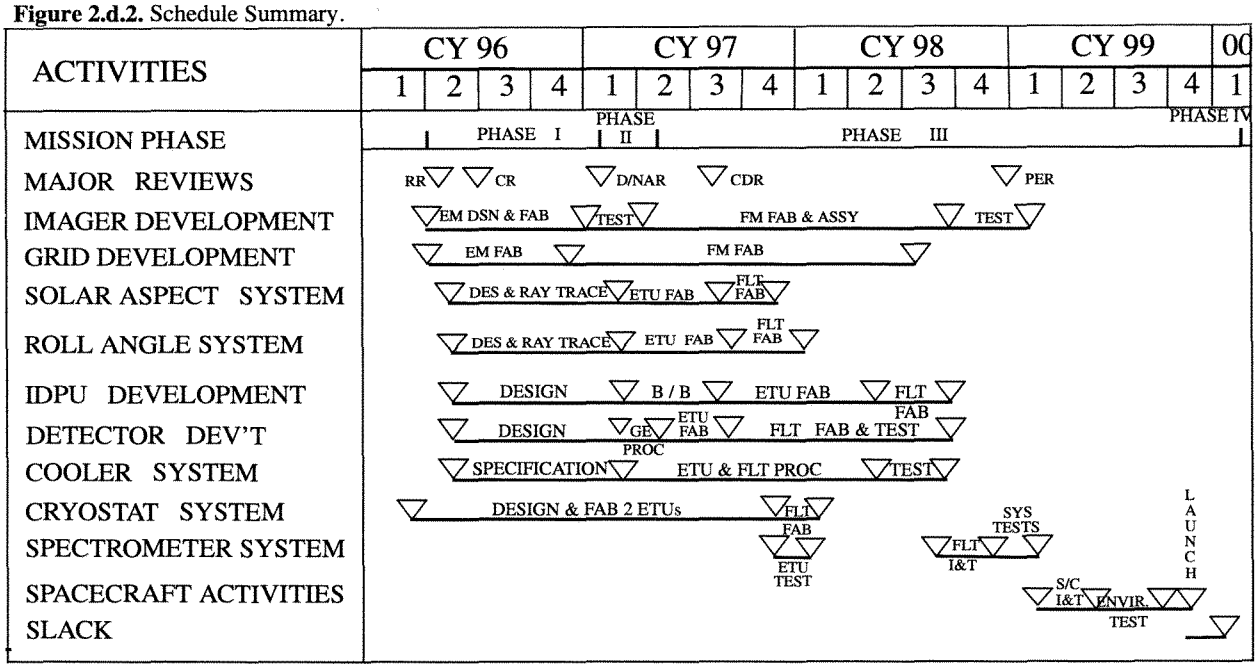

4) CSAs and 5) HVPSs. Each item will undergo qualification vibration and Thermal Vacuum (T/V) testing at the development unit level. Acceptance level vibration and T/V will be done on the flight units prior to delivery to the spacecraft, or following integration into the Spectrometer or Imager systems. Test plans for spare boards and sub-assemblies will be developed on a case by case basis. The SAS electronics with a PC-based GSE are sent to GSFC for integrated into the SAS. The RAS electronics are integrated into the RAS at UCB. The CSAs and HVPSs are integrated into the Spectrometer at UCB.

Software Development

Instrument software development will be done at UCB by the same team which put the first microprocessor controlled instrument in space (ISEE-A Electric Field Instrument) over twenty years ago, and which has had an unbroken string of successes since that time. Software will be written in assembly code and verified by an extensive program of on-orbit-like simulation and testing, using the breadboard and the engineering development IDPU. An ETU IDPU with simulators for the sensors and analog electronics will be maintained through the entire mission flight segment. All software will be thoroughly tested in this system before it is loaded or run in the flight hardware.

The HESSI team's proposed use of the FAST IDPU and processor system with the use by the spacecraft of the FAST MUE will result in a large reduction in software effort - over half of the software modules needed for HESSI can be taken directly from FAST.

Imaging System MI&T

The Imager metering structure and grid trays will be fabricated in the GSFC machine shops based on the techniques successfully developed for the TDU. The coarse grids will also be produced at GSFC using the WEDM technique used for HEIDI. Fine grids will be produced by Delft University of Technology and its subcontractors under the supervision of Co-I van Beek, who developed and patented the required techniques. The SAS optical assemblies will be fabricated and the full-up SAS optically characterized and tested as a complete subsystem at GSFC. The RAS optical assembly is fabricated, integrated with its electronics, and tested as a complete system at UCB.

The assembly, alignment and verification of the Imaging System will be based on proven techniques demonstrated on the TDU, and HEIDI at GSFC; and by Co-I van Beek on his SMM/HXIS experiment. The goals of the assembly, alignment and test plan (Figure 2.d.1) are to (1) initially align the elements of the telescope to the accuracy required to produce efficient X-ray modulation, (2) verify the alignment is maintained during prelaunch testing; (3) provide data on key alignment parameters to optimize imaging performance.

Several alignment facilities have been de-

veloped to assemble and monitor the alignment of the Imaging System. The **Optical Grid Characterization Facility** (OGCF) was used to successfully characterize grids for HEIDI. It uses a CCD video camera to scan a grid mounted on a PC-controlled X-Y table. Image analysis software locates the grid slats with respect to fiducials in the rim and characterizes the mean pitch and uniformity. The **X-Ray Grid Characterization Facility** (XGCF) provides similar information to the OGCF using X-rays to 120 keV. This system uses the Digital Radiography Facility at GSFC. X-ray images of development grids are shown on the foldout.

Grid and SAS components are characterized using a Coordinate Measuring Machine (CMM). The telescope structure is aligned using the Electronic Coordinate Determination System (ECDS), an optical/electronic industrial surveying apparatus. The TMS will monitor relative twist of the grid subassemblies. An optical test of the alignment of the imaging system will be done with the Laser Test GSE at GSFC similar to that used on HEIDI (Gaither *et al.* 1995). Coalignment of the SAS elements is verified by the same technique (solar drift scan) used on HEIDI. This measurement will also establish the cross calibration of the TMS and SAS measurements of tray twist.

The **X-ray Imaging Verification System** will be used as the final test prior to launch to provide end-to-end verification of the performance of the imager by determining the modulation amplitude provided by each grid pair in response to a moving X-ray source. A small, gold-foil 'gridlet' will be used to define the geometry of a 100-microcurie radioactive source of X-rays detectable in both SiDs and GeDs (e.g., ^{109}Cd). For suitable distances from the front grids (typically 1-2 meters), the gridlet geometry is selected so that PC-controlled motion of the gridlet/source produces strong and calculable modulation in the transmitted photon flux through each grid-pair in turn. Data on the X-rays detected with the SiDs and GeDs are recorded through the IDPU. The measured modulation as compared to the expected modulation for each grid pair gives an accurate indication of the overall performance of the Imaging System.

Spectrometer MI&T

UCB will fabricate, integrate, and test the detectors, cold plate and IR/contamination shield, CSAs, HVPS, and all electrical wiring, while GSFC will fabricate the cryostat and test and integrate the cryocooler.

Detectors. The GeDs will be fabricated and tested using the same procedures as for the HIREGS and HEXAGONE instruments. Commercially procured germanium crystal boules are etched, implanted, and segmented into GeDs in the UCB/LBNL GeD fabrication lab. Mechanical parts for the GeD modules are manufactured in the UCB/SSL machine shop with special controls to avoid contamination. Cooled FET CSAs are fabricated by UCB and matched with individual GeDs during testing. Individual GeDs are kept cold in storage cryostats until integration into the spectrometer.

Fabrication of the Si(Li) detectors, including etching, implantation, and manufacture of the detector mounts and the FET preamplifiers will be done at the UCB/LBNL SiD labs.

The detectors are individually calibrated with a set of radioactive γ-ray sources which span the range from soft X-rays to ~2.6 MeV. Energies up to 15 MeV are obtained using neutron-γ sources.

Two engineering test cryostats are fabricated at GSFC; one for thermal and mechanical testing at GSFC with an ETU cooler procured from a commercial vendor, the other for GeD and SiD electrical integration and testing at UCB. Several GeDs and SiDs will be installed early in the engineering test cryostat to evaluate wiring procedures and test for crosstalk, etc. Then a flight cryostat is fabricated at GSFC with the cold plate and IR/contamination shield fabricated at UCB (to control contaminants). The mechanical cryocooler is procured from the same commercial vendor and integrated and tested with the flight cryostat by GSFC.

The cryostat/cooler assembly will then be transferred to the UCB where GeDs and SiDs will be installed and the cryostat purged, evacuated, and cooled. The CSAs and HVPS modules will then be mounted on the cryostat and a complete electrical test done.

Spectrometer-IDPU I&T

The completed IDPU and flight wiring harness will be integrated to the Spectrometer and a full electrical functional test of the Spectrometer assembly performed. Measurements with radioactive sources are then made over a range of angles to calibrate a detailed GEANT Monte Carlo model of the Spectrometer with the precise geometry and materials, as was done for the HIREGS and HEXAGONE instrument.

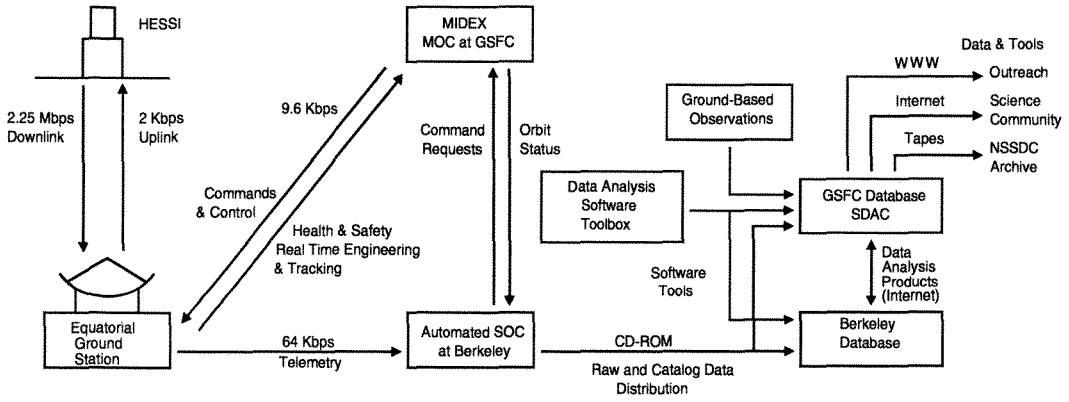

Figure 2.e.1. Mission Operations and Data Analysis Plan

Payload and Spacecraft I&T

The very simple interface between the Imager and the Spectrometer allows them to be fabricated and tested independently and to be brought together for the first time at the spacecraft integration at GSFC. The Imager is first integrated into the spacecraft. A theodolite is used to check that the alignment of the Imaging System to the spacecraft axis is within 0.1°. The TMS test described above is performed again to ensure that no distortion or other damage has occurred to the Imager. The RAS is then integrated to the spacecraft and the alignment measured using standard optical techniques.

Next, the Spectrometer and radiator are installed. Machining tolerances will insure that the Imager and Spectrometer are properly aligned. The IDPU is installed in the spacecraft and a full functional test of the detector system, the SAS, the RAS, and the cooler is done.

Radioactive sources are again used for spectroscopic calibration following integration to obtain total transmission though the grid pairs, confirm the detector calibrations, and assess the effects of the spacecraft on the spectrometer response. These data will be added to the GEANT model, which will be used as the basis for the Spectrometer response in flight. Germanium background lines and an on-board pulser will provide calibrations during flight.

Spacecraft level testing will include a vibration test, acoustics, thermal vacuum, EMC/EMI, and a spin balance. The TMS test will be repeated at selected points in the test flow to ensure that no change in the Imager alignment has occurred.

Following completion of all environmental tests, the X-ray Imaging Verification System will be used with the flight detectors and electronics to collect the data through the IDPU and spacecraft data system to give a complete end-to-end verification of the entire payload.

2.e. MISSION OPERATIONS

The HESSI **mission operations scenario** (Figure 2.e.1) is simple and efficient because both the spacecraft and the instrument are fully autonomous during normal operations. No commands need be sent to the spacecraft for days or even weeks at a time, other than those required to activate the transmitter and dump data during each ground-station pass. Thus, once all spacecraft and instrument functions have been activated and verified after launch, the mission operations scenario consists merely of reading out science data from the onboard memory each orbit and verifying the health and safety of the mission.

We have baselined a single near-equatorial ground station, a NASA- supplied TOTS located at Guam (Figure 2.e.1). We plan to use the NASA-provided Mission Operations Center (MOC) at GSFC, as described in Appendix C of the MIDEX AO, to provide these monitoring functions. Normal MOC activities can be limited to one shift/day. Automated spacecraft and instrument health monitoring at the MOC (an off-site operator is notified in case of a problem) is desirable to minimize possible data loss, but is not required. Mission planning and real-time support is required only during launch and initial orbit acquisition (see Section 2.a.1).

2.f. GROUND DATA SYSTEMS PLAN

TOTS will track and collect data from HESSI for 7-8 minutes every orbit to meet all

telemetry, tracking, and commanding requirements. One deviation from the baseline capabilities offered in the AO is that all data will be sent directly from TOTS to the SOC at UCB over a 64 kbps line to minimize network costs. The SOC will perform the level zero science data processing task (which is minimal for HESSI). The ground station will send commands and strip out the health and safety data to send to the MOC over a 9.6 kbps duplex line. Both the spacecraft software and the ground software will be largely identical to that already developed for FAST, which a UCB SOC and a GSFC MOC.

During Phase I, we intend to further study the ground system cost trade-offs, including alternatives to the TOTS at Guam, possibly a ground station provided by CNES, ESA, or Brazil. Also since both EUVE and FAST are presently considering a combined MOC/SOC at UCB, this will be evaluated for HESSI as well.

2.g. PERFORMANCE ASSURANCE (PA)

The HESSI performance assurance program will be fully compliant with the MIDEX Assurance Requirements (MAR) and Guidelines (MAG), and will be modeled on ANSI/ASQC ISO 9001-1994. All PA will be handled through UCB, allowing the mission office to deal with a single interface to the HESSI team.

The Instrument Project Manager (IPM) will work with the MIDEX office in detailing a Performance Assurance Implementation Plan to apply to flight hardware, flight software, and GSE. PA status will be included in monthly reports and design reviews.

1. Performance Assurance Costs. HESSI has been costed to meet the MAR and MAG. The electronics quality (MIL-883B or better) and fabrication requirements (NHB5300.4) were used in the FAST program and thus we are extremely confident in our cost estimates.

2. Design Reviews. The HESSI team will have informal monthly subsystem reviews alternating between UCB and GSFC. ICDs between the spacecraft and HESSI subsystems will be developed in conjunction with peer reviews at GSFC.

In support of the mission design effort, the HESSI team will support the Requirements and Concept Reviews chaired by the mission team. The PI and Project scientist will lead the effort to refine and document the mission concept and requirements, naturally aided by the instrument design team including expertise from EUVE and FAST.

3. System Safety. The HESSI team will assist the mission team in defining the system safety implementation plan by developing a detailed system description and by supporting safety working group meetings. UCB will document all identified hazards to instrumentation and personnel, hazardous procedures and the methods used to control them. The instrument design will incorporate safety features such as encapsulating high voltages and cryogenic surfaces.

The analyses of hazards during tests, handling and transportation will be addressed at design reviews in subsystem and system-level reviews. All ground procedures used after instrument delivery to the spacecraft will comply with applicable safety restrictions, and all hazardous operations will naturally be identified as such.

4. Design Assurance. Fundamental to the design assurance of HESSI is the experience of the designers involved and the heritage of the systems employed. HESSI system heritage is given in Table 2.b.1.

5. Parts and Materials. Another key to the design is an effective parts and materials program. All HESSI instrument electronics will use the FAST parts list which is MIDEX-compliant and parts screening will follow GSFC 311-INST-001. Parts, materials and limited-life lists will be available to the project from Phase I. Derating will follow PPL App. B. and personnel will maintain records sufficient to implement traceability.

6. Fabrication and Quality Assurance. Printed wiring board fabrication will be subcontracted to one of several suppliers used in FAST. Board cost estimates are based upon S-312-P-003. Coupons will be submitted to GSFC, with a request for one-week turnaround.

All board assembly will proceed in the Electronic Assembly Area, approved for use in EUVE and FAST. Unit testing will occur in ESD-compliant work areas.

Once the flight subsystems are built, logs will be used to verify at least 100 hours of trouble free operation prior to spacecraft integration. Failures will be reported to the MIDEX office and tracked to closure with follow-up analyses and mitigation procedures.

7. Verification Program. The HESSI verification program specifies all tests required to dem-

onstrate that the instrument will meet its requirements in orbit. The Instrument System Engineer develops the program and documents it in the Verification and Environmental test matrix, delivered in Phase I. The test flow is given in Figure 2.d.1.

8. Contamination. In general, the HESSI instrument will require only class 300000 facilities. Tight contamination controls will be required only in the fabrication of the GeDs and their assembly into the Spectrometer. Such controls are in place at UCB/LBNL and have been used for both spacecraft (Wind TGRS) and balloon (HIREGS etc.) instruments.

9. Software Development. HESSI flight and GSE software has considerable heritage from the FAST project (14 of the 21 flight modules and 15 of the 16 GSE modules are directly applicable to HESSI). Software will be part of the instrument design review process, and verification will use the IDPU engineering and flight models, rather than software simulations. Software CM will be performed at UCB. On-orbit command sets will be verified using the engineering model at UCB prior to delivery to the MOC.

2.h. NEW TECHNOLOGY and TECHNOLOGY TRANSFER

The new technology already developed (with NASA funding) and tested for HESSI include: (1) Fine grids made from high-Z materials by foil stacking and WEDM with grid thickness to slat width ratio of ~50:1; (2) Segmented and grounded guard-ring coaxial GeDs; (3) Advanced FETs; (4) Transistor-reset CSAs.

Presently under development are the following enhancements to the Baseline Science Mission: LIGA and other types of grids (NASA and SBIR funded), and silicon drift chambers (joint DOE/industry technology effort). None of these enhancements, however, is required to achieve the Baseline or Minimum Science Mission.

Both the technology items already developed for HESSI and those under development have significant potential for transfer to other NASA missions, the federal government, and the private sector. The transistor-reset CSA circuitry is presently offered by all the major GeD manufacturers in their premium (extra cost) electronic systems. We are considering an offer by a commercial firm (Amptek) to hybridize our CSAs for HESSI in exchange for marketing rights. The guard ring GeDs, transistor reset CSAs, and advanced FETs are currently being considered for the European Space Agency INTEGRAL (INTErnational Gamma-Ray Astrophysics Laboratory) mission as part of NASA's involvement.

Potential fine grid applications (many have been discussed with commercial entities) include X-ray imaging for high volume baggage inspection, characterization of heavy metal deposits, radioactive waste assessment, medical imaging, comb drive actuators and a micro mass spectrometer. The thick film lithography technology for X-ray masks for LIGA may be used to fabricate micro induction coils and channel plates. Both the LIGA and thick film lithography processes will provide an enabling capability for commercialization of a variety of reduced size sensors, instruments and devices.

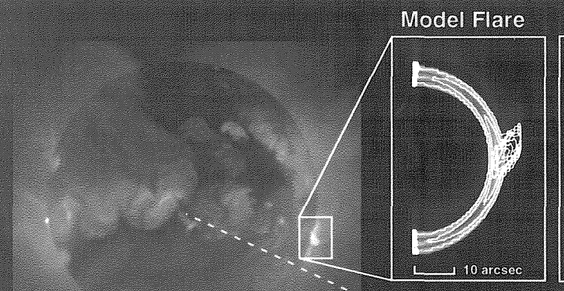

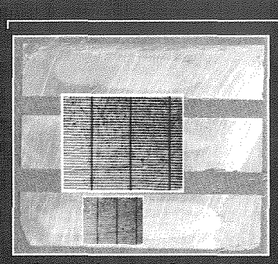

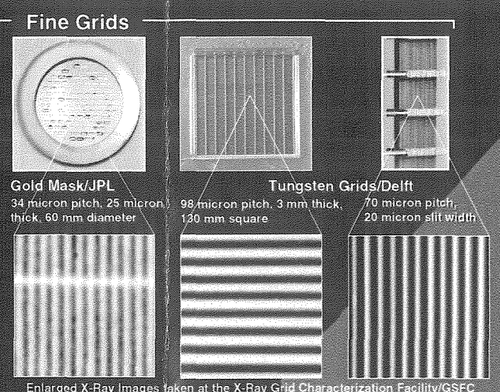

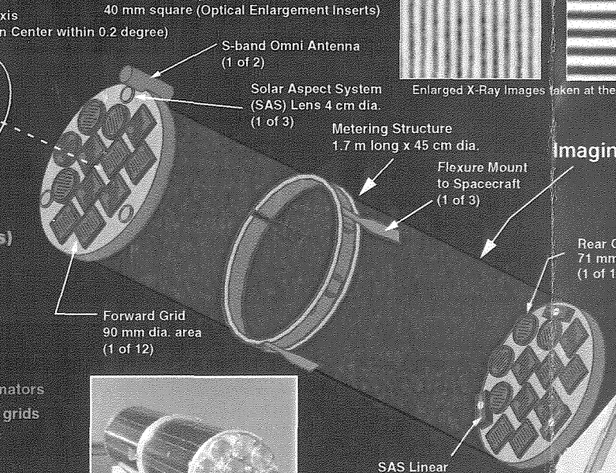

Telescope Demonstration Unit/GSFC
1.7 m long, 45 cm diameter

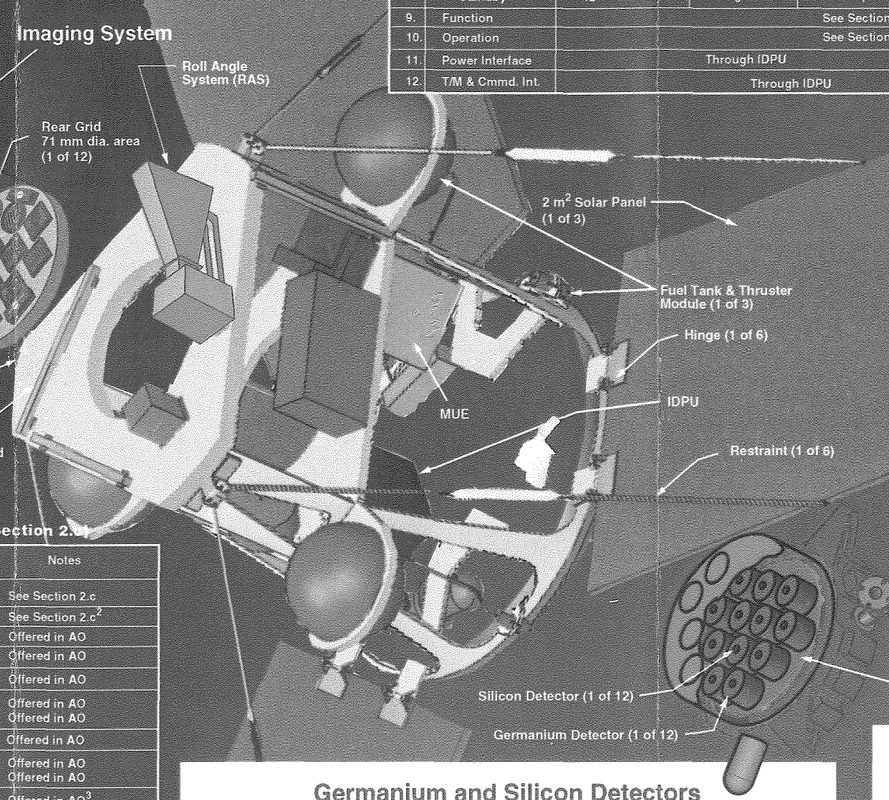

Basic HESSI Instrument Information (see Section 2.b)

		Imaging System		Spectrometer		
		Grids, Trays, Tube, & SAS	RAS	Cryostat, Detectors, Preamps, & HVPSs	Cryocooler and Electronics	IDPU
1.	Size	1.7 m long 45 cm diameter	10 x 10 x 10 cm 30-cm-long shade	30 cm long 50 cm diameter	10 cm dia. x 20 cm 18 cm dia. x 25 cm	27 x 29 x 34 cm
2.	Mass (kg)	64	4	46	14	20
3.	C. of G.	*Center of tube*	*Center of box*	*Center of cyl*	*Centers of each cyl.*	*Center of box*
4.	Shape	Cylinder	Box with Sun-shade	Cylindrical cryostat	Cyl. displacer and compressor	Box
5.	Mechanical Interface with S/C	3-point flexure mount to upper deck	Hard-mount to upper deck	3-point mount to lower deck	Hard mount to lower deck	Hard mount to central deck
6.	Thermal paths	Isolated from spacecraft	Conductive to spacecraft	Isolated from spacecraft	Heat radiated from rear radiator	Conductive cooling to spacecraft deck
7.	FOV	±1° about centerline	±15° perp. to spin axis	±30° about spin axis ±30° perp. to spin axis	None	None
8.	Power (watts):	Heater / SAS				
	Nominal	12 / 2	0.5	6.1	70	60
	Peak	20 / 2	0.5	6.1	70	60
	Duty Cycle (%)	60 / 100	100	100	100	100
	Standby	12 / 0	0	1	70	0
9.	Function	See Section 2b				
10.	Operation	See Section 2b				
11.	Power Interface	Through IDPU			From S/C MUE	
12.	T/M & Cmmd. Int.	Through IDPU				Through MUE

X-ray and Gamma-ray Imaging Spectroscopy

	Baseline Mission	Minimum Science Mission (differences)
Imaging		
• Angular Resolution	2 arcsec to 300 keV	3 arcsec to 50 keV 6 arcsec to 200 keV
Above 1 MeV	20 arcsec	40 arcsec
• Angular Coverage	2 arcsec - 2 arcmin	3 arcsec - 2 arcmin
• Field of View	Full Sun	
• Temporal Resolution	Tens of ms for basic image, 2 s for detailed image	
• Technique	Fourier-transform imaging with rotating modulation collimators	
• Grids	12 tungsten grids	2 gold masks, 5 tungsten grids
• Aspect System	SAS to determine direction to Sun-center to <1.5 arcsec RAS to determine roll angle to <3 arcmin	
Spectroscopy		
Hard X-rays and Gamma-rays		
• Energy Range	10 keV to 20 MeV	
• Energy Resolution	<1 keV FWHM to 1 MeV, increasing to 5 keV at 20 MeV	
• Detectors	Two-segment hyperpure germanium - HPGe	
• Number	12	7
• Dimensions, Temp.	7.1 cm dia. x 8 cm long, cooled to 80K	
Soft X-rays		
• Energy Range	2 to 20 keV	
• Energy Resolution	<1 keV FWHM	
• Detectors	Lithium-drifted silicon - Si(Li)	
• Number	12	7
• Dimensions, Temp.	1 cm dia. x 2 mm thick, cooled to 140K	
Detector Cooling		
• Cryostat	Aluminum Sealed vacuum space with contamination barrier around Ge detectors	
• Cryocooler	Stirling-cycle or pulse-tube options	
• Cooling Power	0.7 watts at 80 K, 1.5 watts at 140 K	
Overall Characteristics		
• Total Instrument Weight	148 kg	130 kg
• Power	151 watts	110 watts
• Telemetry	12 Gbits in 2 days	6 Gbits in 2 days
Special Requirements		
• Orbit: Altitude	600 ± 20 km	
Inclination	<2.5°	<7.5°
• Launch Date	Dec. 1999 preferred as late as Dec. 2001 acceptable	
• *Operational Lifetime*	*2 years, 3rd year highly desirable*	

HESSI Spacecraft Resource Summary (see Section 2.c)

Component		Mass (kg)	Power[1] (watts)	Notes
Structure	Conventional Aluminum	52.0	-	See Section 2.c
C&DH System	FAST MUE	16.0	14.8	See Section 2.c[2]
Shunt Control Boxes		4.5	-	Offered in AO
Transponder	S-Band	4.1	6.5	Offered in AO
Antennas	Two S-Band Omnis	1.5	-	Offered in AO
Solar Array	Three 2m² Si Panels	43.8	-	Offered in AO
	Hinges & Restraints	6.0		Offered in AO
Battery	21 A-H NiCad	23.0	-	Offered in AO
Electrical	Spacecraft Harness	24.0	-	Offered in AO
	Umbilical Assembly	0.5		Offered in AO
Thermal Control	Blankets & Heaters	8.0	0.0	Offered in AO[3]
	Battery Radiator	1.4	-	Offered in AO
	Transponder Heat Sink	1.1	-	*Offered in AO*
Reaction Wheels & Controls	Two 2.8 Nm² Wheels	10.9	16.0	Offered in AO
Propulsion System	Three Hydrazine Thrusters	50.6	-	See Section 2.c
Despin Yo Yo		5.0	-	Launch Function
ACS Components (Electronics in MUE)	Fan Sun Sensor	0.8	0.5	SWAS-FAST Exchange
	Intermediate Sun Sensor	0.3	0.5	Costed to instrument
	Three Axis Magnetometer	0.3	0.2	Offered in AO
	Three 130 Amp m² Bars	5.3	2.0	Offered in AO
Spacecraft Totals		260.1	40.5	
Instrument Totals		148.0	150.6	
HESSI Totals		408.1	191.1	
Med-Lite capability to required orbit		522.0	240.0	
Margins		113.9 21.8%	48.9 20.4%	

[1] Orbit average power
[2] MUE with additional electronics to accommodate the propulsion system
[3] Propulsion system heaters are turned off after all fuel is expelled

Germanium and Silicon Detectors

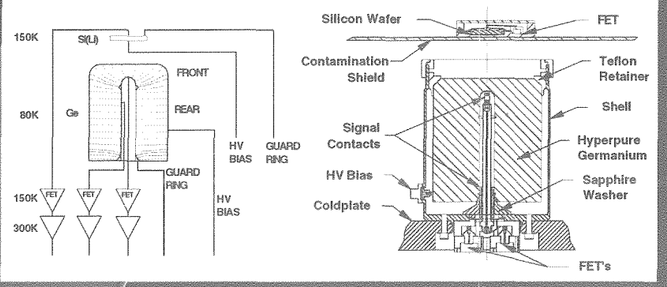

HIREGS Germanium Detector Components

Four HIREGS Germanium Detectors

Cryostat Layout

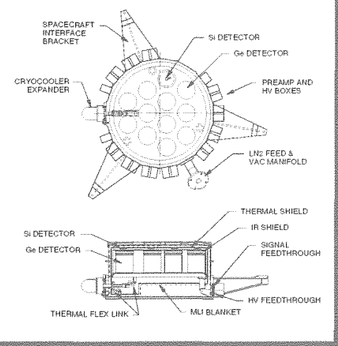

Appendix A. References

Battle, R., and I. Hawkins, 1995. *J. Sci. Educ. & Tech.*, submitted.

Feffer, P. T., R. P. Lin, D. M. Smith, K. C. Hurley, S. R. Kane, S. McBride, J. H. Primbsch, K. Youssefi, G. Zimmer, R. M. Pelling, F. Cotin, J. M. Lavigne, G. Rouaix, S. Slassi, G. Vedrenne, R. Pehl, C. Cork, P. Luke, N. Madden, and D. Malone, 1993. *Astron. Astrophys. Suppl.* **97**, 31.

Gaither, C. C., E. J. Schmahl, C. J. Crannell, B. R. Dennis, F. L. Lang, L. E. Orwig, C. N. Hartman, and G. J. Hurford, 1995. *Applied Optics*, submitted.

Hawkins, I., and R. Battle, 1996. American Education Research Association, April 1996 Symposium, accepted.

Hawkins, I., C. A. Christian, R. Battle, R. F. Malina, and N. Craig, 1994. *Bull. Amer. Astr. Soc.*, **26**, 1311.

Luke, P. N., 1984. *IEEE Trans. Nucl. Sci.* **N5-31**, 312.

Malina, R. F., I. Hawkins, and C. Christian, 1994. Symposium on Space and Education, International Astronautical Congress, Jerusalem, Israel.

Metcalf, T. R., D.L. Mickey, R. C. Canfield, and J. P. Wülser, 1994. In *High Energy Solar Phenomena-A new Era of Spacecraft Measurements*, ed. J. M. Ryan and W. T. Vestrand, *AIP Conf. Proc.* **294**, 59.

Park, I., and M. Hannafin, 1993. *Association for Educational Communications and Technology* **41**, 63-85.

Pelling, M. P. Feffer, K. Hurley, S. Kane, R. Lin, S. McBride, J. Primbsch, D. Smith, K. Youseffi, G. Zimmer, F. Cotin, J. Lavigne, G. Rouaix, S. Slassi, G. Vedrenne, R. Pehl, C. Cork, P. Luke, N. Madden and D. Malone, 1992. In *Proc. SPIE Meeting, San Diego, July 1992,* Society of Photo-Optical Instrumentation Engineers.

Prince, T. A., G. J. Hurford, H. S. Hudson, and C. J. Crannell, 1988. *Solar Phys.*, **118**, 269.

Ramaty, R., N. Mandzhavidze, B, Kozlovsky, and R. J. Murphy, 1995. *Astrophys. J. Lett.*, in press.

Share, G. H., and R. J. Murphy, 1995. *Astrophys. J.*, **452**, 933.

Smith, D. M., R. P. Lin, P. Feffer, S. Slassi, K. Hurley, J. Matteson, H. B. Bowman, R. M. Pelling, M. Briggs, D. Gruber, L. E. Peterson, R. E. Lingenfelter, P. von Ballmoos, I. Malet, M. Niel, G. Vedrenne, P. Durouchoux, P. Wallyn, C. Chapuis, C. Clark, D. Landis, P. Luke, N. Madden, D. Malone and R. Pehl, 1993. *Astrophys. J.* **414**, 165.

Smith, D. M., R. P. Lin, K. A. Anderson, K. Hurley, and C. M. Johns, 1995. *J. Geophys. Res.* **100**, 19675.

van Beek, H. G., P. Hoyng, B. LaFleur, and G. M. Simnett, 1980. *Solar Phys.* **65**, 39.

Wülser, J.-P., Hudson, H. S., Nishio, M., and Kosugi, T., 1995. *Astron. Astrophys.*, submitted.

Appendix B. Acronyms

ACE	Advanced Composition Explorer
ACS	Attitude Control System
ADC	Analog-to-Digital Converter
AH	Amp-Hour
AMPTE	Active Magnetospheric Particle Tracer Explorer
AO	Announcement of Opportunity
ATSR	Along Track Scanning Radiometer on ERS-1 and ERS-2
BAe/MMS	British Aerospace/Matra Marconi Systems
BATSE	Burst and Transient Source Experiment on CGRO
BBSO	Big Bear Solar Observatory, operated by Caltech
BIMA	Berkeley-Illinois-Maryland Array, a radio interferometer in CA
CAD	Computer Aided Design
CAN	Cooperative Agreement Notice
CCD	Charge Coupled Device
CCSDS	Consultative Committee for Space Data Systems
CDR	Critical Design Review
CEA	Center for EUV Astrophysics
CG	Center of Gravity
C&DH	Command and Data Handling
CD-ROM	Compact Disk - Read Only Memory
CGRO	Compton Gamma Ray Observatory
CIS	Cluster Ion Spectrometer, an instrument on each of the CLUSTER Spacecraft
Cluster	Four ISTP spacecraft
CM	Configuration Management
CME	Coronal Mass Ejection
CMM	Coordinate Measuring Machine at GSFC
CNES	Centre National d'Etudes Spatiales (French equivalent of NASA)
COBE	Cosmic Background Explorer
CR	Concept Review
CRRES	Combined Release and Radiation Effects Satellite
CSA	Charge-Sensitive Amplifier
CsI	Cesium Iodide scintillator
Cu	Copper
DC-DC	Direct Current to Direct Current Converter
$\Delta E/E$	Fractional energy resolution
DISCR	Discriminator
DMA	Direct Memory Access
D/NAR	Design/Non-Advocate Review
DoD	Department of Defense
DoE	Department of Energy
ECDS	Electronic Coordinate Determination System
ECO	Engineering Change Order
EEE	Electrical, Electronic, and Electromechanical parts
EEPROM	Electronically Erasable Programmable Read Only Memory
EFI	Electric Field Instrument for Polar spacecraft
EFW	Electric Fields and Waves instrument for Cluster spacecraft
EGRET	Energetic Gamma Ray Experiment on CGRO
ELV	Expendable Launch Vehicle
EM	Engineering Module
EMC	Electro-Magnetic Compatibility
EMI	Electro-Magnetic Interference
EP/EUVE	The EUVE payload sits atop an Explorer Platform (EP) spacecraft
ERS-1 and -2	European Remote Sensing Satellites 1 and 2
ESA	European Space Agency
ESD	ElectroStatic Discharge
ETU	Engineering Test Unit
EUV	Extreme Ultra Violet
EUVE	Extreme Ultra-Violet Explorer
Excel	Microsoft's spreadsheet program
FAST	**F**ast **A**uroral **S**napsho**T** Explorer, a SMEX mission
FET	Field Effect Transistor
FIFO	First-In First-Out
FITS	Flexible Image Transport System, a standard file specification
FM	Flight Module
FMEA	Failure Modes and Effects Analysis
FOV	Field of View
FPGA	Field-Programmable Gate Array
FUSE	Far Ultraviolet Spectroscopic Explorer
FWHM	Full-Width at Half-Maximum
FY	Fiscal Year
GANTT	Timeline chart
Gbytes	Giga bytes (10^9 bytes)
GBO	Ground-Based Observatory

GCF	Grid Characterization Facility
Ge	Germanium
GeD	Germanium Detector
GEANT	A Monte Carlo code for modeling X-ray/Gamma-ray detectors
GeV	Giga (10^9) electron Volts
GEVS	General Environmental Verification Specification (GSFC)
GGS	Global Geospace Science
GOES	NOAA's Geostationary Operational Environmental Satellite
GOES-Next	Follow-on to earlier GOES
GRBM	Gamma-Ray Burst Monitor
GRIS	Gamma-Ray Imaging Spectrometer, a GSFC balloon instrument
GRS	Gamma-Ray Spectrometer on SMM
GSE	Ground-Support Equipment
GSFC	Goddard Space Flight Center
GXRS	Goddard X-Ray Spectrometers on the Argentinian SAC-B Spacecraft
Hα	Optical emission line from atomic hydrogen
HEAO-3	High Energy Astrophysics Observatory-3
HEIDI	High Energy Imaging Device, a GSFC balloon payload
HESI	High Energy Solar Imager, a NASA study that followed HESP
HESP	High Energy Solar Physics mission, a NASA study that preceded HESI
HESSI	High Energy Solar Spectroscopic Imager
HEXAGONE	High Energy X-ray and Gamma-ray Observatory for Nuclear Emissions, a UCB balloon instrument
HIREGS	High Resolution Gamma Ray Spectrometer, a UCB balloon instrument
HIREX	High Resolution X-ray Spectrometer, a UCB balloon instrument
HVPS	High Voltage Power Supply
HXIS	Hard X-ray Imaging Spectrometer on SMM
HXRBS	Hard X-ray Burst Spectrometer on SMM, a GSFC instrument
HXT	Hard X-ray Telescope on Yohkoh
Hz	Hertz
I&T	Integration and Test
I&T&L	Integration and Test and Launch
ICD	Interface Control Document
ID	Identification
IDL	Interactive Data Language from Research Systems, Inc.
IDPU	Instrument Data Processing Unit
IMAX	Manufacturer of the shuttle cabin camera
INTEGRAL	ESA's International Gamma-Ray Astrophysics Laboratory
IPM	Instrument Project Manager
IR	Infra-Red
IRAC	Infrared Array Camera, instrument payload on SIRTF
IRIS	InfraRed Interferometer Spectrometer
IRM	Ion Release Module (an experiment on AMPTE)
ISAMS	Improved Stratospheric and Mesospheric Sounder on UARS
ISE	Instrument Systems Engineer
ISEE	International Sun-Earth Explorer
ISS	Intermediate Sun Sensor
ISTP	International Solar and Terrestrial Physics
JPL	Jet Propulsion Laboratory
kbps	kilo-bits per second
keV	kilo (10^3) electron Volts
KP	Kitt Peak National Observatory
K through 12 (or K-12)	Kindergarten through 12th grade
L	Distance between grids in an RMC
LAN	Local Area Network
LVMS	Local Vertical Measurement System
LBL	Lawrence Berkeley Laboratory
LIGA	Lithografie, Galvanoformung, Abformtechnik (German name for deep-etch X-ray lithography of acrylic resists, electroforming, and replication)
LLD	Lower-Level Discriminator
LN_2	Liquid Nitrogen
LSB	Least-Significant Bit
MAG	MIDEX Assurance Guidelines
MAR	MIDEX Assurance Requirements
Max '91	A joint NASA/NSF program during the 1991 solar maximum.
Mbits	Mega bits (10^6 bits)
Med-Lite	NASA ELV

MET	Mission Elapsed Time
MeV	Mega (10^6) electron Volts
Mil	Military
MI&T	Manufacturing, Integration and Test
MIT	Massachusetts Institute of Technology, Cambridge, MA
MLI	Multi-Layer Insulation
MO&DA	Mission Operations and Data Analysis
MOC	Mission Operations Center
MOLA	Mars Observer Laser Altimeter
MPa	Mega-Pascals, unit of pressure
MSFC	Marshall Space Flight Center
MSM	Minimum Science Mission
MSU	Montana State University
MUE	Mission Unique Electronics
NA or N/A	Not Applicable
NaI	Sodium Iodide (scintillator)
NAOJ	National Astronomical Observatory of Japan
NAR	Non-Advocacy Review
NASA	National Aeronautics and Space Administration
NASTRAN	NASA Structural Analysis program
^{20}Ne	Neon isotope
NHB	NASA Handbook
Ni	Nickel
NiCd or Ni-Cad	Nickel Cadmium
NOAA	National Oceanic and Atmospheric Administration
NRAO	National Radio Astronomy Observatory, Green Bank, WV
NRO	National Radio Observatory
NSF	National Science Foundation
NSO	National Solar Observatory in Tucson, AZ
NSSDC	National Space Science Data Center
OGCF	Optical Grid Characterization Facility
OLS	Orbital Launch Services Project at GSFC
OSSE	Oriented Scintillation Spectrometer Experiment on CGRO
OVRO	Owens Valley Radio Observatory operated by Caltech
p	pitch of a grid
PA	Performance Assurance
PAD	Pitch-Angle Distribution
Pb	Lead
PC	Personal Computer
PCA	Proportional Counter Array on XTE
P-CAD	IBM's PC-based printed circuit layout software
PCB	Printed Circuit Board
Pegasus XL	Launch vehicle built by Orbital Science Corporation
PI	Principal Investigator
PMMA	Polymethyl Methacrylate, an acrylic used in the LIGA process
Polar	Polar Plasma Laboratory, an ISTP spacecraft
PPL	Preferred Parts List
PROM	Programmable Read-Only Memory
PWB	Printed Wiring Board
RAID	Redundant Array of Inexpensive Disks
RAM	Random Access Memory
RAO	Resources Analysis Office at GSFC
RAS	Roll Angle System
REU	Research Experiences for Undergraduates, an NSF Outreach Program
RF	Radio Frequency
RMC	Rotating Modulation Collimator
ROSAT	Roentgen Satellite, a German X-ray telescope
RPA	Réme Plasma Analyzer, an instrument on the Giotto spacecraft to Comet Halley
RPM	Revolutions Per Minute
RR	Requirements Review
RSTN	Radio Solar Telescope Network - USAF
RS232	IEEE interface specification for serial data transfer
S&E	Supplies & Expenses
SAA	South Atlantic Anomaly
SAC-B	Satelite Aplicaciones Scientificas, an Argentinian satellite
SAS	Solar Aspect System on HESSI
SB	Small Business
SBIR	Small Business Innovative Research
SDAC	Solar Data Analysis Center at GSFC
SDB	Small Disadvantaged Business
SEL	NOAA's Space Environment

	Laboratory in Boulder, CO
SEP	Solar Energetic Particle
SERTS	Solar EUV Rocket Telescope and Spectrograph, a GSFC rocket instrument
SHOOT	Superfluid Helium On-Orbit Transfer experiment
Si	Silicon
SiD	Silicon Detector
SIGMA	A Russian satellite
Si(Li)	Lithium-drifted Silicon detector
SII	Science Information Infrastructure
SINDA	Systems Improved Differencing Analyzer (thermal analysis software)
SMEX	Small Explorer
SMM	Solar Maximum Mission (1980-1989)
Sn	Tin
SOC	Science Operations Center
SOHO	Solar and Heliospheric Observatory
SOON	USAF's Solar Optical Observing Network
SP	NSO's Sacramento Peak Observatory
SPEX	X-ray spectroscopy software implemented in IDL at the SDAC
SPRC	Space Physics Research Center
S/R	Shift Register
SR&T	Supporting Research and Technology
SSL	Space Sciences Laboratory at UCB
SSR	Solid-State Recorder
Star 37	Solid rocket motor available as final stage of Med-Lite ELV
STTP	NASA's Solar Terrestrial Theory Program
SUMER	Solar Ultraviolet Measurement of Emitted Radiation on SOHO
SWAS	Submillimeter Wave Astronomy Satellite, SMEX
SXI	Soft X-ray Imager on GOES
SXT	Soft X-ray Telescope on Yohkoh
t	Thickness of a grid
TBD	To Be Determined
TDU	Telescope Demonstration Unit
TGRS	Transient Gamma-Ray Spectrometer on Wind
TM or T/M	Telemetry
TMS	Twist Monitoring System
TOPEX	Topographical Explorer or Ocean Topography Explorer
TOTS	Transportable Orbital Tracking Station
TRASYS	Thermal Radiation Analyzer System (computer program)
TRMM	Tropical Rainfall Measurement Mission
TRW	Thompson Ramo Woolridge Corporation
T/V	Thermal Vacuum
UAH	University of Alabama at Huntsville
UARS	Upper Atmosphere Research Satellite
UC	University of California
UCB	University of California, Berkeley
ULD	Upper-Level Discriminator
UOSAT	University of Surrey satellite
US	United States
USAF	United States Air Force
UV	Ultraviolet
VLA	Very Large Array, radio interferometer at Socorro, NM
w	Grid slit width
W	Watt or the element tungsten
WBS	Work Breakdown Structure
WEDM	Wire Electric Discharge Machine
Wind	An ISTP spacecraft to study the solar wind
WWW	World Wide Web
XDL	Cross Delay Line detector in the Summer instrument on SOHO
XGCF	X-ray Grid Characterization Facility
XTE	X-ray Timing Explorer
Yohkoh	Japanese solar spacecraft launched in 1991
Z	Atomic number or axis in a Cartesian coordinate system
3DP	Three-Dimensional Plasma instrument on Wind spacecraft

High Energy Solar Spectroscopic Imager
HESSI

Science Objective

To explore the basic physics of particle acceleration and explosive energy release in solar flares.

Observational Approach

Observations of X-ray and gamma-ray flares from 2 keV to 20 MeV with an unprecedented combination of high resolution spectroscopy and imaging.

The first hard X-ray imaging spectroscopy.

The first high resolution solar gamma-ray line spectroscopy from space.

The first imaging observations above 100 keV.

The first imaging in narrow gamma-ray lines.

High resolution X-ray and gamma-ray spectra of cosmic sources.

Hard X-ray images of the Crab Nebula with 2 arcsecond resolution.

Primary Observations

Hard X-ray images with an angular resolution as fine as 2 arcseconds, temporal resolution as fine as 10 ms, and energy resolution of <1 keV from 2 keV to >200 keV.

High resolution X-ray and gamma-ray spectra with ~1 keV resolution to energies as high as 20 MeV.

Complementary Observations

Images from the Soft X-ray Imager on GOES.

Energetic particle spectra and abundances from the Advanced Composition Explorer (ACE).

Groundbased radio and optical images, spectra, and magnetograms.

Expected Numbers of Flares

Tens of thousands of microflares.

Thousands of hard X-ray flares with crude imaging and spectra to >100 keV.

Hundreds of flares with $>10^3$ counts s^{-1} above 20 keV allowing spatial changes to be followed on timescales of 0.1 s.

Tens of flares sufficiently intense to allow the finest possible imaging spectroscopy.

Hundreds of flares with the detection of the narrow gamma-ray lines.

Tens of flares with detailed gamma-ray line spectroscopy and the location and extent of the source to 20 arcseconds.

Special Requirements

Pointing to within 0.2° of Sun center.

Spinning at ≥15 rpm.

Equatorial orbit at 600km altittude.

Operations for 2-3 years during next period of high solar activity expected between 1999 and 2003.